

**Modeling of $\Delta^{17}\text{O}$ of
 NO_x and HO_x**

S. Morin et al.

This discussion paper is/has been under review for the journal Atmospheric Chemistry and Physics (ACP). Please refer to the corresponding final paper in ACP if available.

Simulation of the diurnal variations of the oxygen isotope anomaly ($\Delta^{17}\text{O}$) of reactive atmospheric species

S. Morin¹, R. Sander², and J. Savarino³

¹Météo-France/CNRS, CNRM/GAME URA 1357, CEN, 38400 St Martin d'Hères, France

²Air Chemistry Department, Max-Planck Institute of Chemistry, P.O. Box 3060, 55020 Mainz, Germany

³CNRS/Université Joseph Fourier Grenoble 1, LGGE UMR 5183, St Martin d'Hères, France

Received: 22 November 2010 – Accepted: 23 November 2010
– Published: 14 December 2010

Correspondence to: S. Morin (samuel.morin@meteo.fr)

Published by Copernicus Publications on behalf of the European Geosciences Union.

Title Page	
Abstract	Introduction
Conclusions	References
Tables	Figures
◀	▶
◀	▶
Back	Close
Full Screen / Esc	
Printer-friendly Version	
Interactive Discussion	



Abstract

The isotope anomaly ($\Delta^{17}\text{O}$) of secondary atmospheric species such as nitrate (NO_3^-) or hydrogen peroxyde (H_2O_2) has potential to provide useful constrains on their formation pathways. Indeed, the $\Delta^{17}\text{O}$ of their precursors (NO_x , HO_x etc.) differs and depends on their interactions with ozone, which is the main source of non-zero $\Delta^{17}\text{O}$ in the atmosphere. Interpreting variations of $\Delta^{17}\text{O}$ in secondary species requires an in-depth understanding of the $\Delta^{17}\text{O}$ of their precursors taking into account non-linear chemical regimes operating under various environmental settings.

We present results from numerical simulations carried out using the atmospheric chemistry box model (CAABA/MECCA) to explicitly compute the diurnal variations of the isotope anomaly of short-lived species such as NO_x and HO_x . $\Delta^{17}\text{O}$ was propagated from ozone to other species (NO , NO_2 , OH , HO_2 , RO_2 , NO_3 , N_2O_5 , HONO , HNO_3 , HNO_4 , H_2O_2) according to the classical mass-balance equation, through the implementation of various sets of hypotheses pertaining to the transfer of $\Delta^{17}\text{O}$ during chemical reactions.

The model confirms that diurnal variations in $\Delta^{17}\text{O}$ of NO_x are well predicted by the photochemical steady-state relationship during the day, but that at night a different approach must be employed (i.e. "fossilization" of the $\Delta^{17}\text{O}$ of NO_x as soon as the photolytical lifetime of NO_x drops below ca. 5 min). We quantify the diurnally-integrated isotopic signature (DIIS) of sources of atmospheric nitrate and H_2O_2 under the various environmental conditions analyzed, which is of particular relevance to larger-scale implementations of $\Delta^{17}\text{O}$ where high computational costs cannot be afforded.

1 Introduction

Unraveling chemical mechanisms at play in the atmosphere requires finding creative ways to test the predictions of models which describe them. Most studies to date have relied on concentration measurements to validate model results. Over the past

ACPD

10, 30405–30451, 2010

Modeling of $\Delta^{17}\text{O}$ of NO_x and HO_x

S. Morin et al.

Title Page

Abstract

Introduction

Conclusions

References

Tables

Figures

◀

▶

◀

▶

Back

Close

Full Screen / Esc

Printer-friendly Version

Interactive Discussion



Modeling of $\Delta^{17}\text{O}$ of NO_x and HO_x

S. Morin et al.

Title Page

Abstract

Introduction

Conclusions

References

Tables

Figures

◀

▶

◀

▶

Back

Close

Full Screen / Esc

Printer-friendly Version

Interactive Discussion



decades alternative isotopic approaches have demonstrated great capabilities in providing concentration-independent information relevant to atmospheric processes. Of particular interest is the development of measurements of the isotope anomaly ($\Delta^{17}\text{O}$) of oxygen-bearing species (Thiemens, 2006). $\Delta^{17}\text{O}$ is defined as $\delta^{17}\text{O} - 0.52 \times \delta^{18}\text{O}$, with $\delta^x\text{O} = R^x / R_{\text{SMOW}}^x - 1$ ($x=17$ or 18) where R^x refers to the $^{17}\text{O}/^{16}\text{O}$ elemental ratio in the species of interest and in Standard Mean Ocean Water (SMOW), taken as a reference. Ozone (O_3) possesses a unique and distinctive isotope anomaly inherited from mass-independent fractionation during its formation in the atmosphere (Marcus, 2008).

In contrast to conventional isotopic ratios which are affected by isotopic fractionation, $\Delta^{17}\text{O}$ is insensitive to mass-dependent fractionation. Because the vast majority of chemical reaction induce mass-dependent fractionation, $\Delta^{17}\text{O}$ features the remarkable ability to be transferred as is during oxidation reaction in the atmosphere. As a result, $\Delta^{17}\text{O}$ of a given species simply reflects the fractional importance in its elemental composition of oxygen atoms inherited directly or indirectly from ozone. This behavior has opened large possibilities to explore atmospheric oxidation mechanisms using $\Delta^{17}\text{O}$ signatures (Lyons, 2001; Michalski et al., 2003; Thiemens, 2006; Savarino et al., 2000; Savarino and Morin, 2010).

One area of intense research on the interpretation of $\Delta^{17}\text{O}$ signatures is the case of atmospheric nitrate ($\text{HNO}_3 + \text{particulate NO}_3^-$). Indeed, atmospheric nitrate is the final oxidation product of nitrogen oxides ($\text{NO}_x = \text{NO} + \text{NO}_2$), which are of primary importance for air-quality (Jacob, 1999; Finlayson-Pitts and Pitts, 2000; Brown et al., 2006). The development of sensitive methods to analyze the oxygen isotopic composition of nitrate (Michalski et al., 2002; Kaiser et al., 2007) makes it possible to obtain $\Delta^{17}\text{O}$ of atmospheric nitrate at weekly to sub-daily timescales in most environments. This has been used in the recent past to study the seasonal variations in NO_x oxidation pathways in mid-latitudes (Michalski et al., 2003; Tsunogai et al., 2010; Savarino et al., 2010) and polar (Morin et al., 2008, 2009; Kunasek et al., 2008) regions, the nature of the sources of atmospheric nitrate in the Antarctic lower atmosphere (Savarino et al., 2007; McCabe et al., 2007; Frey et al., 2009), and more recently the global-scale vari-

ations in NO_x sink reactions (Alexander et al., 2009). $\Delta^{17}\text{O}$ of nitrate has also been used to identify long-term changes in the oxidative properties of the Earth atmosphere, from centennial (Alexander et al., 2004) to millennial (Erbland et al., 2009) time scales.

While including the isotopic composition of long-lived tracers (e.g. CO_2 , N_2O etc.) into global biogeochemical models of the carbon and nitrogen cycle have proved extremely successful (e.g., Hoag et al., 2005), embedding the $\Delta^{17}\text{O}$ of short-lived reactive compounds into atmospheric photochemical models has only recently gained increased attention (Lyons, 2001; Michalski et al., 2003; Zahn et al., 2006; Dominguez et al., 2009; Gromov et al., 2010; Michalski and Xu, 2010). Current hope within the “atmospheric geochemistry community” is that $\Delta^{17}\text{O}$ data can help solve atmospheric chemistry issues such as ascertaining the relative role of heterogeneous reactions in NO_x sink mechanisms (i.e. what is the exact role of N_2O_5 hydrolysis; Brown et al., 2006). However, inferring quantitative atmospheric information from $\Delta^{17}\text{O}$ of nitrate requires assessing precisely its controls and to include them into a consistent modeling framework. In the last few years, several models have been proposed to study the spatio-temporal variations of $\Delta^{17}\text{O}$ and relate them to spatio-temporal variations of the fractional contribution of NO_x sink reactions. The pioneering work of Lyons (2001) set the stage for the first model study of the seasonal variations of $\Delta^{17}\text{O}$ of atmospheric nitrate by Michalski et al. (2003). Further implementations of $\Delta^{17}\text{O}$ into atmospheric chemistry models were proposed in the following years, from 0D box-modeling (Morin et al., 2008; Dominguez et al., 2009; Michalski and Xu, 2010) to the 3-D chemical transport model GEOS-Chem (Kunasek et al., 2008; Alexander et al., 2009).

This study revisits some assumptions, hypotheses and approaches previously introduced in the literature (e.g. Michalski et al., 2003; Morin et al., 2007, 2008, 2009; Kunasek et al., 2008; Alexander et al., 2009) and puts them within a consistent framework and perspective that makes it easier to understand and implement in existing atmospheric chemistry models. Limitations of the various assumptions that have been used so far are highlighted and critically evaluated. The overarching goal is to provide a rationale behind assumptions and simplifications that have to be used in large scale

Modeling of $\Delta^{17}\text{O}$ of NO_x and HO_x

S. Morin et al.

[Title Page](#)[Abstract](#)[Introduction](#)[Conclusions](#)[References](#)[Tables](#)[Figures](#)[◀](#)[▶](#)[◀](#)[▶](#)[Back](#)[Close](#)[Full Screen / Esc](#)[Printer-friendly Version](#)[Interactive Discussion](#)

model implementation in order to reduce computing costs. First of all, general equations are derived from text-book physical principles. The CAABA/MECCA atmospheric chemistry box model (Sander et al., 2010) was used to explicitly calculate the time evolution of the $\Delta^{17}\text{O}$ of short-lived reactive species at each time step. Model runs were performed in a few simple cases to demonstrate the usefulness of such assessments and provide the basis of future analogous studies. Finally, recommendations are given for the implementation of simplifying assumptions into large-scale atmospheric chemistry models.

2 General framework

2.1 The general “mass-balance” equation

The general “mass-balance” equation (also termed the “continuity equation”) governing the temporal evolution of the concentration of a given species in a given air parcel is given by:

$$\frac{d}{dt}[\text{X}] = \sum_i P_i - \sum_j L_j \quad (1)$$

where P_i (L_j) represents each source (sink) rate [$\text{cm}^{-3}\text{s}^{-1}$] of the species X [cm^{-3}]. Source and sinks include both chemical reactions within the parcel and fluxes at its boundaries. Atmospheric chemistry model are mostly driven by reaction kinetics, so that the chemical components of P_i and L_j are simply expressed as a reaction rate constant (usually referred to as k values) times the relevant atmospheric concentrations (Jacob, 1999; Finlayson-Pitts and Pitts, 2000).

The implementation of $\Delta^{17}\text{O}$ into the mass balance Eq. (1) follows from mass conservation applied to the oxygen isotope anomaly. Of course, this rather simple method would not apply to isotopic enrichment (δ) values, because isotopic fractionation has to be fully taken into account for every reaction considered (Gromov et al., 2010). The key

Modeling of $\Delta^{17}\text{O}$ of NO_x and HO_x

S. Morin et al.

[Title Page](#)[Abstract](#)[Introduction](#)[Conclusions](#)[References](#)[Tables](#)[Figures](#)[◀](#)[▶](#)[◀](#)[▶](#)[Back](#)[Close](#)[Full Screen / Esc](#)[Printer-friendly Version](#)[Interactive Discussion](#)

assumption behind the modeling approach is that sink reaction do not induce a specific mass-independant fractionation, and that every source reaction induce the transfer of a given $\Delta^{17}\text{O}$ value to the newly produced species. The $\Delta^{17}\text{O}$ mass-balance equation reads:

$$5 \quad \frac{d}{dt} \left([X] \times \Delta^{17}\text{O}(X) \right) = \sum_i \left(P_i \times \Delta^{17}\text{O}(X)_i \right) - \left(\sum_j L_j \right) \times \Delta^{17}\text{O}(X) \quad (2)$$

where $\Delta^{17}\text{O}(X)_i$ is the isotope anomaly that is transferred to X through the production channel P_i of the species X. It is estimated as a function of the $\Delta^{17}\text{O}$ value of the precursors involved in a given production channel for species X, using a mass-balance approach based on the counting of the oxygen atoms transferred throughout a given production channel. Mass-independent fractionation induced by a specific reaction can also be taken into account in the equation above. Solving numerically the system of equations formed by Eqs. (1) and (2) for all relevant atmospheric species simultaneously yields the time evolution of the concentration and $\Delta^{17}\text{O}$ of each atmospheric species. This is generally not computationally affordable for large-scale modeling studies such as Alexander et al. (2009). The computation can be carried out for limited periods of time using box models.

2.2 Isotopic exchange reactions

Not only chemical production and destruction impact the $\Delta^{17}\text{O}$ of a given species. Isotopic exchange reactions can also modify it. Their main characteristic is that they have no impact on the chemical budget of a species (i.e., Eq. (1) is not changed), but they have an impact on the isotopic mass-balance Eq. (2). The magnitude of an isotopic exchange reaction can be expressed in a similar manner to chemical production or destruction fluxes. In what follows, the rate of the ℓ isotopic exchange reaction is referred to as IE_ℓ ; the ultimate $\Delta^{17}\text{O}$ value that would be attained in species X if the isotopic exchange with the species Y_ℓ fully proceeds is noted $\Delta^{17}\text{O}(Y_\ell)$. Implementing this into

30410

Modeling of $\Delta^{17}\text{O}$ of NO_x and HO_x

S. Morin et al.

Title Page

Abstract

Introduction

Conclusions

References

Tables

Figures

◀

▶

◀

▶

Back

Close

Full Screen / Esc

Printer-friendly Version

Interactive Discussion



Eq. (2) yields:

$$\begin{aligned} \frac{d}{dt} ([X] \times \Delta^{17}\text{O}(X)) &= \sum_i (P_i \times \Delta^{17}\text{O}(X)_i) \\ &+ \sum_\ell (IE_\ell \times \Delta^{17}\text{O}(Y_\ell)) \\ &- (\sum_j L_j + \sum_\ell IE_\ell) \times \Delta^{17}\text{O}(X) \end{aligned} \quad (3)$$

2.3 Steady-state approximation

A very commonly used simplification in atmospheric chemistry model is the so-called “photochemical steady-state (PSS)” approximation. This simply assumes that the photolytical lifetime of a given species is sufficiently short that the short-term variations of its concentration are negligible, i.e. $\frac{d}{dt}[X] \sim 0$. In other words, a near-perfect balance between sources and sinks for a given species is assumed. Implementing this assumption into the isotopic mass-balance Eq. (2) yields:

$$\Delta^{17}\text{O}(X) = \frac{\sum_i (P_i \times \Delta^{17}\text{O}(X)_i)}{\sum_j L_j} \quad (4)$$

Given that at PSS $\sum_i P_i = \sum_j L_j$, Eq. (4) can be rewritten as follow:

$$\Delta^{17}\text{O}(X) = \frac{\sum_i (P_i \times \Delta^{17}\text{O}(X)_i)}{\sum_i P_i} \quad (5)$$

Stated differently, at PSS the $\Delta^{17}\text{O}$ of a given species is instantaneously equal to the $\Delta^{17}\text{O}$ induced by the combination of its different chemical sources, scaled according to their relative strength, as shown in Eq. (5). Without PSS the time evolution of the $\Delta^{17}\text{O}$ of a given species also takes into account its $\Delta^{17}\text{O}$ value earlier on. The longer the lifetime of a given species, the smoother the time evolution of its $\Delta^{17}\text{O}$.

Title Page

Abstract

Introduction

Conclusions

References

Tables

Figures

◀

▶

◀

▶

Back

Close

Full Screen / Esc

Printer-friendly Version

Interactive Discussion



2.4 Controls on $\Delta^{17}\text{O}$ of atmospheric nitrate and hydrogen peroxide H_2O_2

2.4.1 Atmospheric nitrate

Atmospheric nitrate is formed homogeneously and heterogeneously in the atmosphere through the following reactions (Jacob, 1999; Finlayson-Pitts and Pitts, 2000):



Here, RH represents a generic hydrocarbon. Dry and wet deposition are the main sinks of atmospheric nitrate, controlling its atmospheric lifetime which is on the order of days to weeks (Finlayson-Pitts and Pitts, 2000). A straightforward rearrangement of Eq. (2) yields the equation governing the time evolution of $\Delta^{17}\text{O}$ of atmospheric nitrate:

$$\frac{d}{dt} \left([\text{NO}_3^-] \times \Delta^{17}\text{O}(\text{NO}_3^-) \right) = \quad (6)$$
$$\sum_i \left(P_i \times \Delta^{17}\text{O}(\text{NO}_3^-)_i \right) - \frac{[\text{NO}_3^-]}{\tau} \times \Delta^{17}\text{O}(\text{NO}_3^-)$$

where τ is the atmospheric lifetime of atmospheric nitrate. $\Delta^{17}\text{O}(\text{NO}_3^-)_i$ values can be calculated for each nitrate production channels (Michalski et al., 2003; Morin et al., 2007, 2009; Kunasek et al., 2008):

$$\Delta^{17}\text{O}(\text{NO}_3^-)_{\text{OH}+\text{NO}_2} = 1/3\Delta^{17}\text{O}(\text{OH}) + 2/3\Delta^{17}\text{O}(\text{NO}_2)$$

$$\Delta^{17}\text{O}(\text{NO}_3^-)_{\text{NO}_3+\text{RH}} = \Delta^{17}\text{O}(\text{NO}_3)$$

$$\Delta^{17}\text{O}(\text{NO}_3^-)_{\text{N}_2\text{O}_5} = 5/6\Delta^{17}\text{O}(\text{N}_2\text{O}_5)$$

30412

Title Page

Abstract

Introduction

Conclusions

References

Tables

Figures

◀

▶

◀

▶

Back

Close

Full Screen / Esc

Printer-friendly Version

Interactive Discussion



address variations of $\Delta^{17}\text{O}(\text{NO}_3^-)$ at temporal scale smaller than its atmospheric lifetime (Michalski and Xu, 2010), because sink reactions (both physical and chemical) must then be explicitly taken into account, as shown by Eq. (6).

2.4.2 Hydrogen peroxyde (H_2O_2)

Hydrogen peroxyde is a key atmospheric oxydant which plays a major role for in-cloud oxidation of S(IV) (Finlayson-Pitts and Pitts, 2000; Alexander et al., 2005). Savarino and Thiemens (1999a) demonstrated that it possesses a small but significant $\Delta^{17}\text{O}$ signature, which has then been used to study the partitioning between various S(IV) oxidants in the atmosphere (Savarino et al., 2000; Alexander et al., 2005). H_2O_2 is mostly formed through the self reaction of HO_2 :



5 The $\Delta^{17}\text{O}$ inherited by H_2O_2 during the above reaction is equal to $\Delta^{17}\text{O}(\text{HO}_2)$. The concept of DIIS applies to H_2O_2 in a manner analogous to atmospheric nitrate (see above). Since Reaction (R5) is the sole significant H_2O_2 production pathway, and because the atmospheric lifetime of H_2O_2 is generally larger than one day, the application of Eq. (8) is trivial and shows that seasonal variations of $\Delta^{17}\text{O}(\text{H}_2\text{O}_2)$ can directly be
10 inferred from variations of $\text{DIIS}(\text{HO}_2 + \text{HO}_2)$ at first order.

3 Material and methods: numerical experiments on $\Delta^{17}\text{O}$ of short-lived species

In this study, we focus on the time evolution of the $\Delta^{17}\text{O}$ of short-lived atmospheric reactive species such as HO_x ($\text{OH} + \text{HO}_2$), NO_x ($\text{NO} + \text{NO}_2$) and RO_2 . For simplicity, in this initial study we restrict our analysis to gas-phase reactions and exclude halogen, sulfur and carbonaceous chemistry, to focus on the highly non-linear NO_x - HO_x / RO_x - O_3 chemistry first. The impact of diurnal variations of $\Delta^{17}\text{O}$ of short-lived species on

Modeling of $\Delta^{17}\text{O}$ of NO_x and HO_x

S. Morin et al.

Title Page

Abstract

Introduction

Conclusions

References

Tables

Figures

◀

▶

◀

▶

Back

Close

Full Screen / Esc

Printer-friendly Version

Interactive Discussion



Modeling of $\Delta^{17}\text{O}$ of NO_x and HO_x

S. Morin et al.

Title Page

Abstract

Introduction

Conclusions

References

Tables

Figures

◀

▶

◀

▶

Back

Close

Full Screen / Esc

Printer-friendly Version

Interactive Discussion



secondary species such as atmospheric nitrate and H_2O_2 is explored through the estimation of diurnally-integrated isotopic signature (DIIS) of these species. This method allows to focus on the understanding of the intertwined relationships between $\Delta^{17}\text{O}$ of primary species, and extrapolating their relevance to secondary species using DIIS values, rather than delving into gas/particles interactions which would render obscure some of the behaviors highlighted using the simplified but realistic set of gas-phase reactions summarized in an electronic supplement to this article. This series of 51 reactions (including 14 photolysis reactions) represents a subset of the chemical mechanism implemented in MECCA (Sander et al., 2005) suited for simplified analysis in the remote marine boundary layer.

3.1 Species with constant $\Delta^{17}\text{O}$ values

3.1.1 $\Delta^{17}\text{O}(\text{O}_3)$

The overwhelming source of non-zero $\Delta^{17}\text{O}$ in the atmosphere is ozone (O_3). As repeatedly mentioned in the recent literature (e.g. Morin et al., 2007; Michalski and Bhattacharya, 2009; Alexander et al., 2009; Dominguez et al., 2009), the tropospheric value of $\Delta^{17}\text{O}(\text{O}_3)$ is controversial. In what follows, we use a value for $\Delta^{17}\text{O}(\text{O}_3)$ of 30‰, which falls within the 25–35‰ range generally found in the literature. If $\Delta^{17}\text{O}(\text{O}_3)$ measurements become available in the future, the quantitative conclusions of the present paper in terms of $\Delta^{17}\text{O}$ of any species would simply have to be multiplied by $\Delta^{17}\text{O}(\text{meas. O}_3)/30$, allowing for an easy update of the results presented below. Note that in case diurnal variations of $\Delta^{17}\text{O}(\text{O}_3)$ are discovered and fully documented, the model described below would simply have to be run using a time varying $\Delta^{17}\text{O}(\text{O}_3)$ value, and the results presented below quickly updated.

Ozone is isotopically asymmetrical (Janssen, 2005), i.e. the $\Delta^{17}\text{O}$ borne by its terminal O atoms is higher than at the central position (Bhattacharya et al., 2008; Michalski and Bhattacharya, 2009). In addition, the O atom transferred from O_3 to another

species does not have an equal probability to originate from the central or the terminal position in ozone. To know the value of $\Delta^{17}\text{O}$ transferred through a given bimolecular reaction, it is necessary to know both the intramolecular distribution of $\Delta^{17}\text{O}$ in ozone and the precise mechanistic properties of the chemical reaction (Savarino et al., 2008).

For the following reaction,



the $\Delta^{17}\text{O}$ transfer function was experimentally determined (Savarino et al., 2008):

$$\Delta^{17}\text{O}_{\text{R6}} = 1.18 \times \Delta^{17}\text{O}(\text{O}_3) + 6.6 \quad (9)$$

In what follows we assume that all gas-phase bimolecular chemical reactions involving ozone feature the same mechanistic characteristics. The transferrable $\Delta^{17}\text{O}$ from ozone during such reactions is denoted $\Delta^{17}\text{O}(\text{O}_3^*)$, consistent with Morin et al. (2009) and Alexander et al. (2009). For $\Delta^{17}\text{O}(\text{O}_3) = (30 \pm 5)\%$, this gives $\Delta^{17}\text{O}(\text{O}_3^*) = (42 \pm 6)\%$. In lack of precise measurements of the geographical, seasonal or diurnal variations of $\Delta^{17}\text{O}(\text{O}_3)$, we restrain to using a constant value.

3.1.2 $\Delta^{17}\text{O}(\text{H}_2\text{O})$ and $\Delta^{17}\text{O}(\text{O}_2)$

Because they represent large oxygen reservoirs with a negligible isotope anomaly, we assume in what follows that $\Delta^{17}\text{O}$ of water vapor (H_2O) and molecular oxygen (O_2) are constant, with a value of 0‰ (Barkan and Luz, 2003, 2005).

3.1.3 $\Delta^{17}\text{O}(\text{RO}_2)$

In this study we explicitly separate HO_2 from other peroxy radicals, denoted RO_2 where R represents a carbonaceous chain, because the chemical budget of HO_2 and RO_2 is very different. While reaction involving ozone contribute to the budget of HO_2 , the only source of RO_2 is the reaction between O_2 and a R radical. Since $\Delta^{17}\text{O}(\text{O}_2) = 0\%$

Modeling of $\Delta^{17}\text{O}$ of NO_x and HO_x

S. Morin et al.

[Title Page](#)[Abstract](#)[Introduction](#)[Conclusions](#)[References](#)[Tables](#)[Figures](#)[◀](#)[▶](#)[◀](#)[▶](#)[Back](#)[Close](#)[Full Screen / Esc](#)[Printer-friendly Version](#)[Interactive Discussion](#)

(see above), this immediately implies that $\Delta^{17}\text{O}(\text{RO}_2)=0\text{‰}$ under all tropospheric conditions.

3.2 Overview of the sets of hypotheses regarding the $\Delta^{17}\text{O}$ transfer throughout chemical reactions

5 Below we present the various sets of hypotheses (numbered Cases 1 to 6) implemented to compute the time evolution of $\Delta^{17}\text{O}$ of the species of interest using various assumptions in terms of $\Delta^{17}\text{O}$ transfer.

3.2.1 Case 1: NO_x photochemical steady-state (PSS) and basic hypotheses

- OH, HO_2 : $\Delta^{17}\text{O}$ of both species is equal to 0‰.
- 10 – NO, NO_2 , NO_3 : The $\Delta^{17}\text{O}$ of these species is calculated using PSS:

$$\Delta^{17}\text{O}(\text{NO}_2) = \alpha \times \Delta^{17}\text{O}(\text{O}_3^*)$$

with

$$\alpha = \frac{k_{\text{NO}+\text{O}_3}[\text{O}_3]}{k_{\text{NO}+\text{O}_3}[\text{O}_3] + k_{\text{NO}+\text{HO}_2}[\text{HO}_2] + k_{\text{NO}+\text{RO}_2}[\text{RO}_2]}$$

15 as defined by Michalski et al. (2003) and demonstrated in Morin et al. (2007). It follows from PSS that $\Delta^{17}\text{O}(\text{NO})=\Delta^{17}\text{O}(\text{NO}_2)$. Assuming that the NO_2+O_3 reaction possesses the same mechanistic characteristics as the $\text{NO}+\text{O}_3$ reaction, $\Delta^{17}\text{O}(\text{NO}_3)$ is given as:

$$\Delta^{17}\text{O}(\text{NO}_3) = (2\alpha + 1)/3 \times \Delta^{17}\text{O}(\text{O}_3^*)$$

- HONO, HNO_3 , H_2O_2 : the calculation of $\Delta^{17}\text{O}$ is calculated following Eq. (2).

Title Page

Abstract

Introduction

Conclusions

References

Tables

Figures

◀

▶

◀

▶

Back

Close

Full Screen / Esc

Printer-friendly Version

Interactive Discussion



- N_2O_5 , HNO_4 : both these species are dimers formed by the combinations of two radicals (NO_2 and NO_3 , and NO_2 and HO_2 , respectively). It is assumed in all calculations that photolysis leads to a scrambling of oxygen atoms originally in N_2O_5 and HNO_4 . In this case, the $\Delta^{17}\text{O}$ of the species formed is that of the average $\Delta^{17}\text{O}$ prior to the photolysis. In contrast, thermal decomposition (TD) is not assumed to induce an isotopic scrambling. Thus it is necessary to track the time evolution of the $\Delta^{17}\text{O}$ of both components of the dimer making up N_2O_5 and HNO_4 , respectively, since their O atoms are not isotopically equivalents.

Table 1 gives the $\Delta^{17}\text{O}(\text{X})_i$ values for each species produced, if different from 0 and not given above.

3.2.2 Case 2: explicit NO_x

In this case, the time evolution of $\Delta^{17}\text{O}$ of NO , NO_2 and NO_3 is computed explicitly. This means that the PSS approximation is not used at all regarding the computation of the $\Delta^{17}\text{O}$ of these species. Table 2 presents the chemical reactions for which the $\Delta^{17}\text{O}(\text{X})_i$ is different than in Case 1.

3.2.3 Case 3: explicit HO_x

In this case, in addition to the hypotheses of Case 2 above, the $\Delta^{17}\text{O}$ value of HO_2 is allowed to vary in time and is computed explicitly. This also induces non-zero values of $\Delta^{17}\text{O}(\text{H}_2\text{O}_2)$, through reaction G2110. Table 3 presents the chemical reactions for which the $\Delta^{17}\text{O}(\text{X})_i$ is different than in Case 1 and 2. Note that in Case 3 $\Delta^{17}\text{O}(\text{OH})$ is still assigned a value of 0‰.

3.2.4 Additional tests

In addition to the three main cases presented above, three additional tests were performed. They all are based on Case 3, i.e. they can all be independently compared to

Title Page

Abstract

Introduction

Conclusions

References

Tables

Figures

◀

▶

◀

▶

Back

Close

Full Screen / Esc

Printer-friendly Version

Interactive Discussion



Case 3.

Case 4: MIF H+O₂

In this case, we take into account that reaction H+O₂→HO₂ (G2100) induces mass-independent fractionation of oxygen isotopes. The effect is assumed to be on the order of 1‰, according to Savarino and Thiemens (1999b). In practice, any HO₂ produced through this channel is thus attributed a Δ¹⁷O value of 1‰.

Case 5: thermal decomposition (TD) scrambling

In this case, it is assumed that the thermal decomposition of N₂O₅ and HNO₄ induces a scrambling of their oxygen isotopes. Table 4 presents the chemical reactions for which the Δ¹⁷O(X)_i is different than in Case 1 in terms of Δ¹⁷O_i of species produced upon the thermal decomposition of N₂O₅ and HNO₄.

Case 6: isotopic exchange OH–H₂O

In this case, we take into account the isotopic exchange reaction between OH and H₂O:



where Q denotes one of the three O isotopes. This reaction leads to the erasure of Δ¹⁷O(OH) following isotopic exchange with water vapor, which has a 0‰ Δ¹⁷O. Tropospheric OH is always at photochemical steady-state during daytime given its extremely short lifetime (a few seconds at most). Under such conditions, its Δ¹⁷O is computed as follows:

$$\Delta^{17}O(OH) = \frac{\sum_j L_j}{\sum_j L_j + k_{R7}[OH][H_2O]} \times \Delta^{17}O(OH)_{\text{source}} \quad (10)$$

Title Page

Abstract

Introduction

Conclusions

References

Tables

Figures

◀

▶

◀

▶

Back

Close

Full Screen / Esc

Printer-friendly Version

Interactive Discussion



where values for k_{R7} were measured by Dubey et al. (1997). In this study, the sole chemical reaction considered inducing non-zero $\Delta^{17}\text{O}$ values in OH is the reaction between $\text{O}(^1\text{D})$ and H_2O . Mass-balance then states that $\Delta^{17}\text{O}(\text{OH})_{\text{source}} = 1/2 \times \Delta^{17}\text{O}(\text{O}_3^*)$ (Morin et al., 2007). Under most conditions prevailing in the lower troposphere in mid-latitudes, $\Delta^{17}\text{O}(\text{OH}) = 0\text{‰}$ (Michalski et al., 2003). However, under cold conditions the isotopic exchange reaction can compete with its OH chemical sinks (Morin et al., 2007), which are mostly $\text{OH} + \text{CH}_4$ and $\text{OH} + \text{CO}$ (Finlayson-Pitts and Pitts, 2000). When Case 6 is tested, $\Delta^{17}\text{O}(\text{OH})$ is assigned a value calculated from Eq. (10) and the mixing ratio of CO , CH_4 and H_2O and the relevant kinetic rate constants.

3.3 Numerical implementation and computation of $\Delta^{17}\text{O}$

MECCA

MECCA (Model Efficiently Computing the Chemistry of the Atmosphere, Sander et al., 2005) is embedded in the CAABA (Chemistry As A Box-model Application, Sander et al., 2010) bundle. It uses an adaptative time resolution mathematical method to solve the stiff set of equations describing the evolution of the chemical composition of the portion of atmosphere hypothetically contained in a closed box.

Isotopic equations

The MECCA box-model described just above, like all atmospheric chemistry models, solves the continuity equation for all considered species and all reactions simultaneously:

$$\frac{d}{dt}[\text{X}] = \sum_i P_i - \sum_j L_j$$

Considering that the model provides the necessary data at a time step t , it follows that at the next time step $t + \Delta t$:

$$[\text{X}](t + \Delta t) = [\text{X}](t) + \Delta t \times \sum_i P_i - \Delta t \times \sum_j L_j \quad (11)$$

30420

Title Page

Abstract

Introduction

Conclusions

References

Tables

Figures

◀

▶

◀

▶

Back

Close

Full Screen / Esc

Printer-friendly Version

Interactive Discussion



The same applies to the isotopic continuity equation (Eq. 2), so that:

$$\begin{aligned} [X](t + \Delta t) \times \Delta^{17}\text{O}(X)(t + \Delta t) &= [X](t) \times \Delta^{17}\text{O}(X)(t) \\ &+ \Delta t \times \sum \left(P_i \times \Delta^{17}\text{O}(X)_i(t) \right) \\ &- \Delta t \times \left(\sum_j L_j \right) \times \Delta^{17}\text{O}(X)(t) \end{aligned} \quad (12)$$

By combining Eqs. (11) and (12), $\Delta^{17}\text{O}(X)(t + \Delta t)$ can be inferred as a function of the relevant chemical and isotopic data at time t . This simple explicit approach was implemented in a computer program separate from MECCA, which takes as input a data file containing the variables dealt with in Eqs. (11) and (12) at each time step, and processes them according to the different cases described above in terms of $\Delta^{17}\text{O}(X)_i$ to compute the time evolution of $\Delta^{17}\text{O}$ of each relevant species.

One major issue that has to be considered when using this simple approach pertains to the comparison of the chemical lifetime of a species X and the time-step of the integration of Eqs. (11) and (12). Indeed, if the lifetime of X is shorter than the time step considered, then the total chemical production or destruction during a given time step Δ may exceed the amount of species X dealt with in the box (or grid-cell). This causes immediate failure of the integration procedure. The time step of the isotopic calculations performed here was chosen accordingly. A time resolution of 10s was found to be sufficient to avoid integration issues such as described above. More integrated approaches, fully embedded into the box-model itself, have been developed and avoid such shortcomings (see e.g., Gromov et al., 2010). However, for the sake of the present study, and taking advantage of the easiness of manipulating $\Delta^{17}\text{O}$ through simple mass-balance equations, we preferred the implementation presented above for this study.

3.4 Presentation of MECCA model runs

Our base-run corresponds to atmospheric settings typical of the remote, mid-latitude (45° N) boundary layer during springtime. Photolysis rate coefficients are calculated

Modeling of $\Delta^{17}\text{O}$ of NO_x and HO_x

S. Morin et al.

Title Page

Abstract

Introduction

Conclusions

References

Tables

Figures

◀

▶

◀

▶

Back

Close

Full Screen / Esc

Printer-friendly Version

Interactive Discussion



Modeling of $\Delta^{17}\text{O}$ of NO_x and HO_x

S. Morin et al.

[Title Page](#)[Abstract](#)[Introduction](#)[Conclusions](#)[References](#)[Tables](#)[Figures](#)[◀](#)[▶](#)[◀](#)[▶](#)[Back](#)[Close](#)[Full Screen / Esc](#)[Printer-friendly Version](#)[Interactive Discussion](#)

as a function of solar zenith angle using a simple parameterization. The model run is started on 1 April, at a temperature of 293 K, a relative humidity of 81%, with a starting NO_2 mixing ratio of 20 pmol mol^{-1} . Initial values for the mixing-ratio of main atmospheric species follow: CH_4 , $1.8 \text{ } \mu\text{mol mol}^{-1}$; CO , 70 nmol mol^{-1} ; H_2O_2 , $600 \text{ pmol mol}^{-1}$; HNO_3 , 5 pmol mol^{-1} ; HCHO , 30 pmol mol^{-1} ; O_3 , 25 nmol mol^{-1} . After a spin-up time of 1 day, sufficient to initialize the mixing ratio of short-lived species, the time evolution of the mixing ratio and isotope anomaly of short-lived species is analyzed during 36 h, corresponding to the time frame between 24 and 60 h from the start of the model run. In lack of emissions of primary species into the box considered, this suffices to identify and study the main features of the diurnal variations of the mixing ratio and $\Delta^{17}\text{O}$ of short-lived species while not suffering from the inherent limitations of box-modeling experienced when longer time periods are considered (Sander et al., 2005).

We concentrate our in-depth analysis on this one model run, which shows many different interesting features of the diurnal variations of $\Delta^{17}\text{O}$ of short-lived species and their sensitivity of the various assumptions tested through Cases 1 to 6. The intricacy and the highly non-linear coupling between HO_x , NO_x including their $\Delta^{17}\text{O}$ requires careful attention to decipher the causes for the variation of $\Delta^{17}\text{O}$. The relevance of the conclusions reached from this analysis is assessed using other model runs undertaken under different atmospheric conditions. Indeed, atmospheric chemical processes depend in particular on temperature, time of the year and latitude (through their control of incoming solar radiation) and the chemical regime of the atmosphere.

4 Results

4.1 Description and analysis of the base model run

4.1.1 Diurnal variations in mixing ratios and reaction rates

Figure 2 shows the diurnal evolution of the mixing ratio of O_3 , HO_x and NO_x/NO_y (NO_y refers to NO_x and its reservoir species such as NO_3 , N_2O_5 , HNO_4 etc.) simulated by MECCA under the conditions of the base model run presented in Sect. 3.4. It shows typical variations, notably with peak values of OH, HO_2 and NO reached during the day. The NO_x/NO_y partitioning changes diurnally, with species such as NO_3 and N_2O_5 present mostly during the night, and species such as HNO_4 , HONO present mostly during the day. H_2O_2 is produced during the day, and undergoes dry deposition which leads to a reduction of its mixing ratio during the night. The mixing ratio of ozone remains quasi-constant during the time period studied, illustrating that the simulation reproduces fairly well the chemical steady-state prevailing in the remote, mid-latitude boundary layer.

As a straightforward corollary of the above paragraph, it appears that within the simulation the $OH+NO_2$ and HNO_4 hydrolysis are mostly daytime nitrate production pathways, while NO_3+RH and N_2O_5 hydrolysis proceed only at night, when significant amounts of NO_3 and N_2O_5 are present. Note that this study does not aim at disentangling complex aspects of the daytime chemistry of N_2O_5 revealed by recent field campaigns (e.g., Brown et al., 2006). H_2O_2 is only produced during the day, when HO_2 maximizes. Figure 3 exemplifies such opposed behavior and illustrates the concept behind diurnally-integrated isotopic signature (DIIS) of the nitrate and hydrogen peroxide sources. From the analysis of this figure, it appears obvious that the nighttime $\Delta^{17}O$ values of HO_2 have no impact on the $\Delta^{17}O$ of H_2O_2 produced. Only daytime $\Delta^{17}O$ values are worth discussing in this case.

Modeling of $\Delta^{17}O$ of NO_x and HO_x

S. Morin et al.

Title Page

Abstract

Introduction

Conclusions

References

Tables

Figures

◀

▶

◀

▶

Back

Close

Full Screen / Esc

Printer-friendly Version

Interactive Discussion



4.1.2 Overview of the diurnally-integrated isotopic signatures (DIIS) values for atmospheric nitrate and hydrogen peroxyde

Table 5 shows the DIIS values for the four atmospheric nitrate sources considered, as well as for H_2O_2 . The main results of this simulation are that

- DIIS values for the $\text{OH}+\text{NO}_2$ reaction pathway are on the order of 20‰ and do not seem significantly dependent to within 0.1‰ upon the different isotopic assumptions tested, except Case 5 which is detailed below. In particular, whether $\Delta^{17}\text{O}(\text{NO}_2)$ is computed explicitly or using the PSS formula has no impact on the DIIS value.
- DIIS values for HNO_4 hydrolysis are on the order of 16‰ and do not depend on the method to compute the $\Delta^{17}\text{O}$ of NO_x (Case 1 and Case 2 yield similar results). When $\Delta^{17}\text{O}(\text{HO}_2)$ is computed explicitly, HNO_4 DIIS values increase moderately by ca. 0.6‰.
- DIIS values for NO_3+RH and N_2O_5 hydrolysis are on the order of 40 and 33‰, respectively, and show a significant different between Case 1 and Case 2, i.e. whether PSS is used to compute the $\Delta^{17}\text{O}$ of NO_x and NO_y . Using the PSS formulation for NO_x yields an overestimation of 1.8‰ of the DIIS values for both nitrate production channels.
- DIIS values for H_2O_2 production are 0 for both Cases 1 and 2, consistent with the fact that $\Delta^{17}\text{O}(\text{HO}_2)$ is assigned a value of 0. When $\Delta^{17}\text{O}(\text{HO}_2)$ is computed explicitly, the DIIS value reaches 1.1‰ (Case 3). Taking into account mass-independent fraction (MIF) of 1‰ in the $\text{H}+\text{O}_2$ reaction leads to increasing the DIIS value by 0.7‰.
- under the environmental conditions tested, whether isotopic exchange between OH and H_2O is considered has no significant impact on all the reaction pathways

Title Page

Abstract

Introduction

Conclusions

References

Tables

Figures

◀

▶

◀

▶

Back

Close

Full Screen / Esc

Printer-friendly Version

Interactive Discussion



considered. This simply indicates that $\Delta^{17}\text{O}(\text{OH})=0\%$ under these environmental conditions.

- Isotopic scrambling during the thermal decomposition of N_2O_5 and HNO_4 leads to lowering the DIIS value of all reaction pathways, excepted H_2O_2 production.

4.1.3 Detailed analysis of the main results

Representation of diurnal variations of $\Delta^{17}\text{O}(\text{NO}_2)$

As shown on Fig. 3a, $\Delta^{17}\text{O}(\text{NO}_2)$ exhibits diurnal variations with a maximum during the night and a minimum during the day, consistent with previous expectations (Morin, 2009). Figure 4 compares the results obtained using permanent photochemical steady-state (Case 1, NO_x PSS) and explicitly computed (Case 2, NO_x explicit, see Sect. 3.2.2). During the day, both calculations show a minimum at noon, on the order of 28%. This is explained by the fact that during the day, the contribution of the $\text{NO}+\text{RO}_2$ and $\text{NO}+\text{HO}_2$ to the production of NO_2 peaks at noon, when peroxy radicals reach their maximum values (see Fig. 2). Owing to the short lifetime of NO_2 during the day, the result of the computation based on PSS is fully consistent with the explicit computation. This explains why the DIIS value for the $\text{OH}+\text{NO}_2$ pathway is the same under Case 1 and Case 2 (see Table 5), because this pathway operates only during the day, when $\Delta^{17}\text{O}(\text{NO}_2)$ has the same value whether Case 1 or Case 2 is considered.

The major difference between the two simulations occurs at night. Indeed, while the result from PSS leads $\Delta^{17}\text{O}(\text{NO}_2)$ to reach values above 41% at night (i.e., on the order of $\Delta^{17}\text{O}(\text{O}_3^*)$), the result from the explicit calculation does not exceed 39% at night, except for a limited period of time at dawn. The explanation for this behavior follows: at dusk, the $\Delta^{17}\text{O}(\text{NO}_2)$ is fixed by the PSS conditions which prevail just before PSS recycling of NO_x becomes insignificant. At this point, NO_2 becomes relatively inert and its $\Delta^{17}\text{O}$ does not vary anymore. As evidenced by Fig. 4, night-time $\Delta^{17}\text{O}(\text{NO}_2)$ corresponds to the $\Delta^{17}\text{O}(\text{NO}_2)$ value computed at PSS when the lifetime of NO_2 is on

Title Page

Abstract

Introduction

Conclusions

References

Tables

Figures

◀

▶

◀

▶

Back

Close

Full Screen / Esc

Printer-friendly Version

Interactive Discussion



the order of 10 min. It is then “fossilized” until the dawn comes, along with the restart of photochemical activity. The difference between the two calculations lies between 2 and 3‰ under the conditions of the base model run. This explains why DIIS values for the nighttime nitrate production pathways depend strongly on the method chosen to compute $\Delta^{17}\text{O}(\text{NO}_x)$ and $\Delta^{17}\text{O}(\text{NO}_y)$, because much of the difference occurs at night.

$\Delta^{17}\text{O}(\text{HO}_2)$ and $\Delta^{17}\text{O}(\text{H}_2\text{O}_2)$

In Cases 3, 4, 5 and 6, where $\Delta^{17}\text{O}(\text{HO}_2)$ is computed explicitly, non-zero $\Delta^{17}\text{O}(\text{HO}_2)$ values are simulated. Figure 5 shows the diurnal variations of $\Delta^{17}\text{O}(\text{HO}_2)$ and $\Delta^{17}\text{O}(\text{H}_2\text{O}_2)$. The non-zero $\Delta^{17}\text{O}$ value in Case 3, on the order of 1‰, stems directly from the $\text{OH}+\text{O}_3$ reaction producing HO_2 with a non-zero $\Delta^{17}\text{O}$ value, which is then mixed with other sources of HO_2 . The addition of mass-independent fractionation through the $\text{H}+\text{O}_2$ reaction, which is dominant HO_2 production reaction, results in elevating the $\Delta^{17}\text{O}(\text{HO}_2)$ value by roughly the magnitude of the isotopic fractionation constant. Combining the explicit calculation of the time evolution of $\Delta^{17}\text{O}(\text{HO}_2)$ with the inclusion of mass-independent fractionation occurring during the $\text{H}+\text{O}_2$ reaction leads to daytime $\Delta^{17}\text{O}(\text{HO}_2)$ values on the order of 2‰.

We note that the corresponding DIIS values relevant to H_2O_2 production for either Case 3 or 4 (1.1 and 1.8‰, respectively) is consistent with the experimental results of Savarino and Thiemens (1999a), who measured rainwater $\Delta^{17}\text{O}(\text{H}_2\text{O}_2)$ values ranging between 1.2 and 2.4‰, under coastal California conditions.

Impact of isotopic scrambling during the thermal decomposition of N_2O_5 and HNO_4

Case 5 tests the hypothesis where thermal decomposition leads to isotopic scrambling between O atoms in molecules making up N_2O_5 and HNO_4 (see Table 4). Under such conditions, it is observed that the $\Delta^{17}\text{O}$ of HO_2 increases, while $\Delta^{17}\text{O}$ of NO_x gener-

Modeling of $\Delta^{17}\text{O}$ of NO_x and HO_x

S. Morin et al.

Title Page

Abstract

Introduction

Conclusions

References

Tables

Figures

◀

▶

◀

▶

Back

Close

Full Screen / Esc

Printer-friendly Version

Interactive Discussion



ally decreases. This behavior is reflected in the DIIS values of the relevant reactions (see Table 5). Detailed investigation of the reasons for this result reveals that much of the effect proceeds through the thermal decomposition of HNO_4 , especially at dusk when HNO_4 thermal decomposition is on the order of its formation rate due to reduced photochemical activity lowering the amount of HO_2 . Through slow but steady cycles of formation/decomposition, HNO_4 temporarily bridges the pool of oxygen atoms within NO_x and HO_x , leading to lowering the $\Delta^{17}\text{O}$ of NO_x and increasing the $\Delta^{17}\text{O}$ of HO_x in a significant manner (see Fig. 5). The same holds for N_2O_5 in terms of oxygen atoms swapping, but this effect is less visible owing to other existing coupling mechanisms between NO_x and NO_3 . In the following, we do not further discuss the impact of the hypothesis of Case 5, although model results are also given for this case.

4.2 Sensitivity to atmospheric conditions

This section presents the results obtained under different conditions than in the base model run. For the sake of brevity, and since the physico-chemical reasons behind the observed behavior are similar to the phenomena described above, we focus our attention on DIIS values, which provide an efficient metrics to compare model runs carried out under different environmental conditions.

4.2.1 Impact of seasonal variations

Using the same chemical mechanism and the same initial chemical composition of the boundary layer, model runs were performed at different times of the year, i.e. starting from 1 January with a temperature of 283 K and 1 July with a temperature of 303 K to see whether seasonal variations in environmental conditions (temperature and actinic flux) can modify the conclusions reached above for the springtime model run, started on 1 April with a temperature of 293 K. The photochemical activity increases monotonically from the winter to summer model runs, as expected (chemical data not shown).

Modeling of $\Delta^{17}\text{O}$ of NO_x and HO_x

S. Morin et al.

Title Page

Abstract

Introduction

Conclusions

References

Tables

Figures

◀

▶

◀

▶

Back

Close

Full Screen / Esc

Printer-friendly Version

Interactive Discussion



The model shows that the DIIS of daytime nitrate production (OH+NO₂ and HNO₄ hydrolysis) is most dependent on the season, due to its strong ties to photochemical activity, which controls Δ¹⁷O of NO₂ and HNO₄ through photochemical steady state during the day. The DIIS of OH+NO₂ varies significantly, from ca. 17‰ in summer to ca. 25‰ during the winter. The DIIS of HNO₄ photolysis also varies, from ca. 14‰ in summer to ca. 19‰ in winter.

In contrast, the DIIS of nighttime nitrate production channels exhibits a stronger dependence upon the isotopic assumption (as detailed in Sect. 4.1.3), but shows little seasonal variations. The biggest variation is between Case 1 (using PSS applied to NO_x) and Case 2 (explicit Δ¹⁷O(NO_x) throughout the day), the former leading to an overestimation ranging from 1.3 to 1.9‰, from winter to summer for both N₂O₅ hydrolysis and NO₃+RH. The DIIS of nighttime nitrate production channels varies within about 1‰ seasonally, on the order of 40 (32.5)‰ year-round, for the NO₃+RH (N₂O₅ hydrolysis) channel.

Last, the DIIS of H₂O₂ production shows little seasonal variation (less than 0.1‰). It is consistently on the order of 1‰ when only the OH+O₃ reaction is responsible for Δ¹⁷O transfer from O₃ to HO₂. It increases to around 1.7‰ when mass-independent fractionation of 1‰ is considered throughout the reaction H+O₂ → HO₂. The only major change occurs in Case 5, i.e. considering scrambling during the thermal decomposition of N₂O₅ and HNO₄.

Under the conditions experienced for our base model run, the isotopic exchange reaction between OH and H₂O does not lead to Δ¹⁷O(OH) values significantly different from 0. This explains why the DIIS values for Case 6 are very similar to that of Case 3. This effects becomes significant only at lower temperatures (see Morin et al., 2007) and is further explored in Sect. 4.2.2.

Modeling of Δ¹⁷O of NO_x and HO_x

S. Morin et al.

Title Page

Abstract

Introduction

Conclusions

References

Tables

Figures

I◀

▶I

◀

▶

Back

Close

Full Screen / Esc

Printer-friendly Version

Interactive Discussion



4.2.2 Higher latitude and colder conditions

A simulation was carried out under springtime Arctic conditions, i.e. a latitude of 80° N and temperature of 253 K, starting from 1 April. The results of this comparison is shown in terms of DIIS values in Table 7.

The DIIS values of daytime nitrate production channels show a strong difference between Arctic and mid-latitude conditions. With the exception of Case 6, the Arctic DIIS values for the OH+NO₂ reaction are ca. 5.5‰ higher than at mid-latitudes, which simply stems from reduced photochemical recycling under reduced insolation prevailing in the Arctic and colder temperatures. It is noteworthy that under Arctic conditions, owing to the lower temperatures prevailing, the OH+NO₂ DIIS value is 2‰ higher under Case 6 (isotopic exchange between OH and H₂O) than under other cases (except Case 5). The diurnal variations of Δ¹⁷O(NO₂) is similar for Case 2 and Case 6 under Arctic conditions, demonstrating that all of the difference observed stems from the fact that Δ¹⁷O(OH) amounts ca. 6‰ under Arctic conditions and Case 6, consistent with the initial estimates provided by Morin et al. (2007).

The DIIS values for nighttime nitrate production are very similar under mid-latitude and Arctic conditions, on the order of 40‰ and 33‰, for NO₃+RH and N₂O₅ hydrolysis, respectively. Note also that the impact of the hypothesis of Case 6 on the DIIS values is insignificant. In terms of H₂O₂ DIIS, Arctic values tend to be a little lower by a few tenths of ‰. The effect of Case 6 is limited to 0.1‰ in terms of H₂O₂ DIIS.

In summary, the impact of colder and more boreal environmental conditions is mostly seen for the DIIS of daytime nitrate production, upon which photochemical conditions and the Δ¹⁷O of OH have a direct impact. The DIIS of nighttime nitrate production channels as well as H₂O₂ seem to be fairly insensitive to these factors.

4.2.3 Higher initial NO_x mixing ratio

A further simulation was carried out under springtime mid-latitude conditions (45° N, 293 K), with an initial NO_x mixing ratio of 2 μmol mol⁻¹ instead of 20 pmol mol⁻¹ in the

Title Page

Abstract

Introduction

Conclusions

References

Tables

Figures

◀

▶

◀

▶

Back

Close

Full Screen / Esc

Printer-friendly Version

Interactive Discussion



base run. The results in terms of DIIS are shown in Table 8. The impact of performing the PSS approximation to compute $\Delta^{17}\text{O}$ of NO_x is similar, i.e. the impact is non-existing for daytime nitrate production pathways and H_2O_2 , and more visible in the case of nighttime nitrate production pathways, although the difference between Case 1 and Case 2 for nighttime nitrate production pathways is smaller than under the conditions of the base model run. Due to enhanced photochemical activity fueled by higher initial NO_x levels, the DIIS values for $\text{OH}+\text{NO}_2$ are reduced by 3‰ when higher initial NO_x levels are set. The impact on nighttime nitrate production channels is limited, with DIIS values on the order of 40‰ (34‰) for NO_3+RH (N_2O_5 hydrolysis) reactions, varying less than 1‰ across this strong chemical gradient.

5 Discussion and implications

5.1 Implications for modeling $\Delta^{17}\text{O}(\text{NO}_3^-)$

We compare here our results to the implementation of $\Delta^{17}\text{O}(\text{NO}_3^-)$ into the GEOS-CHEM chemistry transport model, which was recently carried out by Alexander et al. (2009). In this work, $\Delta^{17}\text{O}(\text{NO}_x)$ was computed under the hypothesis of photochemical steady-state. For the sole daytime nitrate production channel considered ($\text{OH}+\text{NO}_2$), $\Delta^{17}\text{O}(\text{NO}_2)$ was computed using the α value (see Sect. 3.2.1) computed using accumulated reaction rates between 10:00 and 14:00 solar time. For nighttime nitrate production channels, Alexander et al. (2009) used the photochemical steady-state formalism using NO_2 production rates accumulated between 0:00 and 2:00 solar time. We compute the $\Delta^{17}\text{O}$ inherited by atmospheric nitrate through the $\text{OH}+\text{NO}_2$ and NO_3+RH using the algorithm of Alexander et al. (2009) presented above, and compare it to the DIIS values. The results are given in Table 9. We find that the algorithm introduced by Alexander et al. (2009) underestimates the isotopic signature of the $\text{OH}+\text{NO}_2$ channel by 1‰, because it ignores contributions of this channel before 10:00 and after 14:00, when $\Delta^{17}\text{O}(\text{NO}_2)$ is relatively higher than during noontime but the $\text{OH}+\text{NO}_2$ reaction

Title Page

Abstract

Introduction

Conclusions

References

Tables

Figures

◀

▶

◀

▶

Back

Close

Full Screen / Esc

Printer-friendly Version

Interactive Discussion



proceeds significantly. Alexander et al. (2009) also overestimate the isotopic signature of the NO_3+RH channel by 1.6‰, due to the fact that they use PSS equations to derive $\Delta^{17}\text{O}(\text{NO}_y)$ at night, which has been proven above to cause significant overestimation of the DIIS of nighttime nitrate production channels.

We strongly suggest that DIIS values are implemented in large-scale modeling frameworks, such as GEOS-CHEM, to avoid performing such errors. The daytime issue can be resolved using α values computed in a similar manner than in Alexander et al. (2009) but over a larger integration period (e.g., at least from 6:00 to 18:00 solar time). The issue with the nighttime nitrate production channels should be solved without resorting to using photochemical steady state equations at night, since we have shown that this leads to systematically erroneous results and is based on a scientific oxymoron. Given the apparent low sensitivity of DIIS values for nighttime nitrate production channels to environmental conditions such as temperature, actinic flux and NO_x levels, a conservative approach may be to use a fixed value of 40 and 33‰ value for the DIIS of NO_3+RH and N_2O_5 hydrolysis, respectively.

5.2 Implication for $\Delta^{17}\text{O}(\text{H}_2\text{O}_2)$

An interesting implication of our work is the fact that under all tested environmental conditions, the model predicts non-zero $\Delta^{17}\text{O}(\text{H}_2\text{O}_2)$ even without invoking mass-independent fractionation through the $\text{H}+\text{O}_2$ reaction, as evidenced by Savarino and Thiemens (1999a). This significant $\Delta^{17}\text{O}(\text{H}_2\text{O}_2)$, on the order of 1‰, stems from the $\text{OH}+\text{O}_3$ reaction and could be used in the future to probe the level of photochemical activity of a given air parcel through measurements of $\Delta^{17}\text{O}(\text{H}_2\text{O}_2)$ either in the gas-phase or in rainwater, as suggested by Savarino and Thiemens (1999b).

5.3 Open questions

Two untested assumptions of this work are the hypothesis that $\Delta^{17}\text{O}(\text{O}_3)$ remains constant throughout the day and, and that the thermal decomposition of N_2O_5 and HNO_4

Modeling of $\Delta^{17}\text{O}$ of NO_x and HO_x

S. Morin et al.

Title Page

Abstract

Introduction

Conclusions

References

Tables

Figures

◀

▶

◀

▶

Back

Close

Full Screen / Esc

Printer-friendly Version

Interactive Discussion



does not lead to any isotopic scrambling between the two molecules making up these dimers. The assumption related to the diurnal variations of $\Delta^{17}\text{O}(\text{O}_3)$ should be addressed in the near future using field measurements carried out using a chemical probing method based upon the $\text{NO}_2^- + \text{O}_3$ reaction (Michalski and Bhattacharya, 2009; Vicars and Savarino, 2010). The question related to the chemical mechanism operating during thermal decomposition requires advanced chemical physics modeling at the molecular scale. Alternatively, studies on $\Delta^{17}\text{O}(\text{H}_2\text{O}_2)$ may partly solve this issue, since we have shown that the DIIS of its production is most sensitive to this assumption.

6 Conclusions

This study addresses in detail the question of the impact of diurnal variations of $\Delta^{17}\text{O}$ of short-lived reactive species on secondary species such as atmospheric nitrate and H_2O_2 . Using a state of the art photochemical box model, the time evolution of $\Delta^{17}\text{O}$ of NO_x , NO_y and HO_x is computed under various sets of hypotheses pertaining to the method of computing the $\Delta^{17}\text{O}$ values, reflecting different levels of simplifying approximations. Most of the conclusions of this article are drawn from model simulations carried out under clean atmospheric conditions in mid-latitudes ; their broader relevance and robustness is however assessed using model simulations carried out under cold and boreal conditions, and under a 100-fold increase in initial NO_x mixing ratio.

The primary goal of this study was to demonstrate that using a detailed box-modeling study to assess the isotopic signature of various nitrate and H_2O_2 production pathways is feasible and provides relevant information to larger-scale modeling studies. In the meantime, essential features of the coupling between chemical reactions and the $\Delta^{17}\text{O}$ of key atmospheric species were described and are most likely also valid under different environmental contexts. Taking this study as an initial step, the model could rather easily be extended to account for gas/particles interactions, which are of primary importance for the budget of NO_x , and to simulate $\Delta^{17}\text{O}$ values of secondary species such as atmospheric nitrate and H_2O_2 under atmospheric contexts as different as over conti-

Title Page

Abstract

Introduction

Conclusions

References

Tables

Figures

◀

▶

◀

▶

Back

Close

Full Screen / Esc

Printer-friendly Version

Interactive Discussion



nents (urban polluted, tropical etc.) and under polar conditions including more complex and realistic chemical mechanisms. We believe that the present study provides the necessary framework for carrying out this work under conditions that will make it usable by larger-scale modeling studies, or for the interpretation of short-term intensive measurement campaigns using a modeling tool analogous to CAABA/MECCA.

Supplementary material related to this article is available online at:
[http://www.atmos-chem-phys-discuss.net/10/30405/2010/
acpd-10-30405-2010-supplement.pdf](http://www.atmos-chem-phys-discuss.net/10/30405/2010/acpd-10-30405-2010-supplement.pdf).



The publication of this article is financed by CNRS-INSU.

References

- Alexander, B., Savarino, J., Kreutz, K. J., and Thiemens, M. H.: Impact of preindustrial biomass-burning emissions on the oxidation pathways of tropospheric sulfur and nitrogen, *J. Geophys. Res.*, 109, D08303, doi:10.1029/2003JD004218, 2004. 30408
- Alexander, B., Park, R. J., Jacob, D. J., Li, Q. B., Yantosca, R. M., Savarino, J., Lee, C. C. W., and Thiemens, M. H.: Sulfate formation in sea-salt aerosols: constraints from oxygen isotopes, *J. Geophys. Res.*, 110, D10307, doi:10.1029/2004JD005659, 2005. 30414
- Alexander, B., Hastings, M. G., Allman, D. J., Dachs, J., Thornton, J. A., and Kunasek, S. A.: Quantifying atmospheric nitrate formation pathways based on a global model of the oxygen isotopic composition ($\Delta^{17}\text{O}$) of atmospheric nitrate, *Atmos. Chem. Phys.*, 9, 5043–5056, doi:10.5194/acp-9-5043-2009, 2009. 30408, 30410, 30415, 30416, 30430, 30431, 30446

Title Page

Abstract

Introduction

Conclusions

References

Tables

Figures

◀

▶

◀

▶

Back

Close

Full Screen / Esc

Printer-friendly Version

Interactive Discussion



- Barkan, E. and Luz, B.: High-precision measurements of $^{17}\text{O}/^{16}\text{O}$ and $^{18}\text{O}/^{16}\text{O}$ of O_2 and O_2/Ar ratios in air, *Rapid Commun. Mass Sp.*, 17(24), 2809–2814, 2003. 30416
- Barkan, E. and Luz, B.: High-precision measurements of $^{17}\text{O}/^{16}\text{O}$ and $^{18}\text{O}/^{16}\text{O}$ ratios in H_2O , *Rapid Commun. Mass Sp.*, 19, 3737–3742, 2005. 30416
- 5 Bhattacharya, S. K., Pandey, A., and Savarino, J.: Determination of intramolecular isotope distribution of ozone by oxidation reaction with silver metal, *J. Geophys. Res.*, 113, D03303, doi:10.1029/2006JD008309, 2008. 30415
- Brown, S. S., Ryerson, T. B., Wollny, A. G., Brock, C. A., Peltier, R., Sullivan, A. P., Weber, R. J., Dubé, W. P., Trainer, M., Meagher, J. F., Fehsenfeld, F. C., and Ravishankara, A. R.: Variability in nocturnal nitrogen oxide processing and its role in regional air quality, *Science*, 311, 67–70, doi:10.1126/science.1120120, 2006. 30407, 30408, 30423
- 10 Dominguez, G., Wilkins, G., and Thiemens, M. H.: A photochemical model and sensitivity study of the triple-oxygen isotopic ($\Delta^{17}\text{O}$) composition of NO_y , HO_x , and H_2O_2 in a polluted boundary layer, *Atmos. Chem. Phys. Discuss.*, 9, 13355–13406, doi:10.5194/acpd-9-13355-2009, 2009. 30408, 30415
- 15 Dubey, M. K., Mohrschladt, R., Donahue, N. M., and Anderson, J. G.: Isotope specific kinetics of hydroxyl radical (OH) with water (H_2O): testing models of reactivity and atmospheric fractionation, *J. Phys. Chem. A*, 101, 1494–1500, 1997. 30420
- Erbland, J., Savarino, J., Morin, S., and Frey, M. M.: The oxygen isotope anomaly ($\Delta^{17}\text{O}$) of nitrate in the Vostok ice core: insights in possible changes in NO_x oxidation pathways over the last 150 000 years, *Geophys. Res. Abstract*, 11, EGU–2009–975, talk, 2009. 30408
- 20 Finlayson-Pitts, B. J. and Pitts, J. N.: *Chemistry of the upper and lower atmosphere: theory, experiments and applications*, Academic Press, San Diego, CA, 2000. 30407, 30409, 30412, 30414, 30420
- 25 Frey, M. M., Savarino, J., Morin, S., Erbland, J., and Martins, J. M. F.: Photolysis imprint in the nitrate stable isotope signal in snow and atmosphere of East Antarctica and implications for reactive nitrogen cycling, *Atmos. Chem. Phys.*, 9, 8681–8696, doi:10.5194/acp-9-8681-2009, 2009. 30407
- Gromov, S., Jöckel, P., Sander, R., and Brenninkmeijer, C. A. M.: A kinetic chemistry tagging technique and its application to modelling the stable isotopic composition of atmospheric trace gases, *Geosci. Model Dev.*, 3, 337–364, doi:10.5194/gmd-3-337-2010, 2010. 30408, 30409, 30421
- 30 Hoag, K. J., Still, C. J., Fung, I. Y., and Boering, K. A.: Triple oxygen isotope composition of

Modeling of $\Delta^{17}\text{O}$ of NO_x and HO_x S. Morin et al.

[Title Page](#)[Abstract](#)[Introduction](#)[Conclusions](#)[References](#)[Tables](#)[Figures](#)[◀](#)[▶](#)[◀](#)[▶](#)[Back](#)[Close](#)[Full Screen / Esc](#)[Printer-friendly Version](#)[Interactive Discussion](#)

Modeling of $\Delta^{17}\text{O}$ of NO_x and HO_x

S. Morin et al.

Title Page

Abstract

Introduction

Conclusions

References

Tables

Figures

◀

▶

◀

▶

Back

Close

Full Screen / Esc

Printer-friendly Version

Interactive Discussion



tropospheric carbon dioxide as a tracer of terrestrial gross carbon fluxes, *Geophys. Res. Lett.*, 32, L02802, doi:10.1029/2004GL021011, 2005. 30408

Jacob, D. J.: Introduction to Atmospheric Chemistry, Princeton University Press, Princeton, NJ, USA, 1999. 30407, 30409, 30412

5 Janssen, C.: Intramolecular isotope distribution in heavy ozone ($^{16}\text{O}^{18}\text{O}^{16}\text{O}$ and $^{16}\text{O}^{16}\text{O}^{18}\text{O}$), *J. Geophys. Res.*, 110, D08308, doi:10.1029/2004JD005479, 2005. 30415

Kaiser, J., Hastings, M. G., Houlton, B. Z., Röckmann, T., and Sigman, D. M.: Triple oxygen isotope analysis of nitrate using the denitrifier method and thermal decomposition of N_2O , *Anal. Chem.*, 79, 599–607, doi:10.1021/ac061022s, 2007. 30407

10 Kunasek, S. A., Alexander, B., Steig, E. J., Hastings, M. G., Gleason, D. J., and Jarvis, J. C.: Measurements and modeling of $\Delta^{17}\text{O}$ of nitrate in snowpits from Summit, Greenland, *J. Geophys. Res.*, 113, D24302, doi:10.1029/2008JD010103, 2008. 30407, 30408, 30412

Lyons, J. R.: Transfer of mass-independent fractionation in ozone to other oxygen-containing radicals in the atmosphere, *Geophys. Res. Lett.*, 28, 3231–3234, 2001. 30407, 30408

15 Marcus, R. A.: Mass-independent oxygen isotope fractionation in selected systems. Mechanistic considerations, *Adv. Quantum Chem.*, 55, 5–19, doi:10.1016/S0065-3276(07)00202-X, 2008. 30407

McCabe, J. R., Thiemens, M. H., and Savarino, J.: A record of ozone variability in South Pole Antarctic snow: the role of nitrate oxygen isotopes, *J. Geophys. Res.*, 112, D12303, doi:10.1029/2006JD007822, 2007. 30407

20 Michalski, G. and Bhattacharya, S. K.: The role of symmetry in the mass independent isotope effect in ozone, *P. Natl. Acad. Sci. USA*, 106, 5493–5496, doi:10.1073/pnas.0812755106, 2009. 30415, 30432

Michalski, G. and Xu, F.: Isotope modeling of nitric acid formation in the atmosphere using ISO-RACM: testing the importance of NO oxidation, heterogeneous reactions, and trace gas chemistry, *Atmos. Chem. Phys. Discuss.*, 10, 6829–6869, doi:10.5194/acpd-10-6829-2010, 2010. 30408, 30414

25 Michalski, G., Savarino, J., Böhlke, J. K., and Thiemens, M. H.: Determination of the total oxygen isotopic composition of nitrate and the calibration of a $\Delta^{17}\text{O}$ nitrate reference material, *Anal. Chem.*, 74, 4989–4993, doi:10.1021/ac0256282, 2002. 30407

30 Michalski, G., Scott, Z., Kabling, M., and Thiemens, M. H.: First measurements and modeling of $\Delta^{17}\text{O}$ in atmospheric nitrate, *Geophys. Res. Lett.*, 30, 1870, doi:10.1029/2003GL017015, 2003. 30407, 30408, 30412, 30413, 30417, 30420

Modeling of $\Delta^{17}\text{O}$ of NO_x and HO_x

S. Morin et al.

[Title Page](#)
[Abstract](#)
[Introduction](#)
[Conclusions](#)
[References](#)
[Tables](#)
[Figures](#)
[Back](#)
[Close](#)
[Full Screen / Esc](#)
[Printer-friendly Version](#)
[Interactive Discussion](#)


- Morin, S.: Interactive comment on “Quantifying atmospheric nitrate formation pathways based on a global model of the oxygen isotopic composition ($\Delta^{17}\text{O}$) of atmospheric nitrate” by B. Alexander et al., *Atmos. Chem. Phys. Discuss.*, 9, C1154–C1170, 2009. 30425
- Morin, S., Savarino, J., Bekki, S., Gong, S., and Bottenheim, J. W.: Signature of Arctic surface ozone depletion events in the isotope anomaly ($\Delta^{17}\text{O}$) of atmospheric nitrate, *Atmos. Chem. Phys.*, 7, 1451–1469, doi:10.5194/acp-7-1451-2007, 2007. 30408, 30412, 30415, 30417, 30420, 30428, 30429
- Morin, S., Savarino, J., Frey, M. M., Yan, N., Bekki, S., Bottenheim, J. W., and Martins, J. M. F.: Tracing the origin and fate of NO_x in the Arctic atmosphere using stable isotopes in nitrate, *Science*, 322, 730–732, doi:10.1126/science.1161910, 2008. 30407, 30408
- Morin, S., Savarino, J., Frey, M. M., Domine, F., Jacobi, H. W., Kaleschke, L., and Martins, J. M. F.: Comprehensive isotopic composition of atmospheric nitrate in the Atlantic Ocean boundary layer from 65°S to 79°N , *J. Geophys. Res.*, 114, D05303, doi:10.1029/2008JD010696, 2009. 30407, 30408, 30412, 30416
- Sander, R., Kerkweg, A., Jöckel, P., and Lelieveld, J.: Technical note: The new comprehensive atmospheric chemistry module MECCA, *Atmos. Chem. Phys.*, 5, 445–450, doi:10.5194/acp-5-445-2005, 2005. 30415, 30420, 30422
- Sander, R., Gromov, S., Harder, H., Jöckel, P., Kerkweg, A., Kubistin, D., Riede, H., Taraborrelli, D., and Tost, H.: The atmospheric chemistry box model CAABA/MECCA-3.0, *Geosci. Model Dev. Discuss.*, in preparation, 2010. 30409, 30420
- Savarino, J. and Morin, S.: Handbook of Environmental Isotope Geochemistry, chap. 44, The N, O, S isotopes of oxy-anions in ice cores and polar environments, Springer-Verlag, New York, in preparation, 2010. 30407
- Savarino, J. and Thiemens, M. H.: Analytical procedure to determine both $\delta^{18}\text{O}$ and $\delta^{17}\text{O}$ of H_2O_2 in natural water and first measurements, *Atmos. Environ.*, 33, 3683–3690, 1999a. 30414, 30426, 30431
- Savarino, J. and Thiemens, M. H.: Mass-independent oxygen isotope (^{16}O , ^{17}O and ^{18}O) fractionation found in H_x , O_x reactions, *J. Phys. Chem. A*, 103, 9221–9229, 1999b. 30419, 30431
- Savarino, J., Lee, C. C. W., and Thiemens, M. H.: Laboratory oxygen isotopic study of sulfur(IV) oxidation: Origin of the mass-independent oxygen isotopic anomaly in atmospheric sulfates and sulfate mineral deposits on Earth, *J. Geophys. Res.*, 105, 29079–29088, doi:10.1029/2000JD900456, 2000. 30407, 30414

- Savarino, J., Kaiser, J., Morin, S., Sigman, D. M., and Thiemens, M. H.: Nitrogen and oxygen isotopic constraints on the origin of atmospheric nitrate in coastal Antarctica, *Atmos. Chem. Phys.*, 7, 1925–1945, doi:10.5194/acp-7-1925-2007, 2007. 30407
- 5 Savarino, J., Bhattacharya, S. K., Morin, S., Baroni, M., and Doussin, J.-F.: The NO+O₃ reaction: a triple oxygen isotope perspective on the reaction dynamics and atmospheric implications for the transfer of the ozone isotope anomaly, *J. Chem. Phys.*, 128, 194303, doi:10.1063/1.2917581, 2008. 30416
- 10 Savarino, J., Morin, S., Erbland, J., Grannec, F., Patey, M. D., and Achterberg, E. P.: Seasonal variations of isotopic ratios of atmospheric nitrate in the tropical Atlantic Ocean (Cape Verde Observatory, 16° N), *Geophys. Res. Lett.*, in preparation, 2010. 30407
- Thiemens, M. H.: History and applications of mass-independent isotope effects, *Annu. Rev. Earth Pl. Sc.*, 34, 217–262, doi:10.1146/annurev.earth.34.031405.125026, 2006. 30407
- 15 Tsunogai, U., Komatsu, D. D., Daita, S., Kazemi, G. A., Nakagawa, F., Noguchi, I., and Zhang, J.: Tracing the fate of atmospheric nitrate deposited onto a forest ecosystem in Eastern Asia using $\Delta^{17}\text{O}$, *Atmos. Chem. Phys.*, 10, 1809–1820, doi:10.5194/acp-10-1809-2010, 2010. 30407
- Vicars, W. and Savarino, J.: A method to measure diurnal variations of the isotope anomaly ($\Delta^{17}\text{O}$) of tropospheric ozone, *Anal. Chem.*, in preparation, 2010. 30432
- 20 Zahn, A., Franz, P., Bechtel, C., Groß, J.-U., and Röckmann, T.: Modelling the budget of middle atmospheric water vapour isotopes, *Atmos. Chem. Phys.*, 6, 2073–2090, doi:10.5194/acp-6-2073-2006, 2006. 30408

**Modeling of $\Delta^{17}\text{O}$ of
NO_x and HO_x**

S. Morin et al.

[Title Page](#)[Abstract](#)[Introduction](#)[Conclusions](#)[References](#)[Tables](#)[Figures](#)[◀](#)[▶](#)[◀](#)[▶](#)[Back](#)[Close](#)[Full Screen / Esc](#)[Printer-friendly Version](#)[Interactive Discussion](#)

Modeling of $\Delta^{17}\text{O}$ of NO_x and HO_x

S. Morin et al.

Table 1. Listing of $\Delta^{17}\text{O}(\text{X})_i$ relevant to Case 1, if not given in Sect. 3.2.1. Note the special case of HNO_4 and N_2O_5 , for which the $\Delta^{17}\text{O}$ of each of the molecule making up the dimer are explicitly referred to and tracked.

Rxn #		$\Delta^{17}\text{O}(\text{X})_i$
G3109	$\text{NO}_3 + \text{NO}_2 \rightarrow \text{N}_2\text{O}_5$	$\Delta^{17}\text{O}(\text{N}_2\text{O}_5 - \text{NO}_2)_{\text{G3109}} = \Delta^{17}\text{O}(\text{NO}_2)$ $\Delta^{17}\text{O}(\text{N}_2\text{O}_5 - \text{NO}_3)_{\text{G3109}} = \Delta^{17}\text{O}(\text{NO}_3)$
G3200	$\text{NO} + \text{OH} \rightarrow \text{HONO}$	$\Delta^{17}\text{O}(\text{HONO})_{\text{G3200}} = 1/2 \left(\Delta^{17}\text{O}(\text{NO}) + \Delta^{17}\text{O}(\text{OH}) \right)$
G3202	$\text{NO}_2 + \text{OH} \rightarrow \text{HNO}_3$	$\Delta^{17}\text{O}(\text{HNO}_3)_{\text{G3202}} = 1/3 \left(2\Delta^{17}\text{O}(\text{NO}_2) + \Delta^{17}\text{O}(\text{OH}) \right)$
G3203	$\text{NO}_2 + \text{HO}_2(+\text{M}) \rightarrow \text{HNO}_4$	$\Delta^{17}\text{O}(\text{HNO}_4 - \text{NO}_2)_{\text{G3203}} = \Delta^{17}\text{O}(\text{NO}_2)$
G4109	$\text{HCHO} + \text{NO}_3(+\text{O}_2) \rightarrow \text{HNO}_3 + \text{CO} + \text{HO}_2$	$\Delta^{17}\text{O}(\text{HNO}_3)_{\text{G4109}} = \Delta^{17}\text{O}(\text{NO}_3)$

Title Page

Abstract

Introduction

Conclusions

References

Tables

Figures

◀

▶

◀

▶

Back

Close

Full Screen / Esc

Printer-friendly Version

Interactive Discussion



Table 2. $\Delta^{17}\text{O}(\text{X})_i$ for Case 2: explicit NO_x . Only equations featuring different $\Delta^{17}\text{O}(\text{X})_i$ than in Case 1 are presented here.

Rxn #		$\Delta^{17}\text{O}(\text{X})_i$
G3103	$\text{NO} + \text{O}_3 \rightarrow \text{NO}_2 + \text{O}_2$	$\Delta^{17}\text{O}(\text{NO}_2)_{\text{G3103}} = 1/2 \left(\Delta^{17}\text{O}(\text{O}_3^*) + \Delta^{17}\text{O}(\text{NO}) \right)$
G3106	$\text{NO}_2 + \text{O}_3 \rightarrow \text{NO}_3 + \text{O}_2$	$\Delta^{17}\text{O}(\text{NO}_3)_{\text{G3106}} = 1/2 \left(\Delta^{17}\text{O}(\text{O}_3^*) + \Delta^{17}\text{O}(\text{NO}_2) \right)$
G3108	$\text{NO}_3 + \text{NO} \rightarrow 2\text{NO}_2$	$\Delta^{17}\text{O}(\text{NO}_2)_{\text{G3108}} = 1/2 \left(\Delta^{17}\text{O}(\text{NO}_3) + \Delta^{17}\text{O}(\text{NO}) \right)$
G3110	$\text{N}_2\text{O}_5 (+\text{M}) \rightarrow \text{NO}_2 + \text{NO}_3$	$\Delta^{17}\text{O}(\text{NO}_2)_{\text{G3110}} = \Delta^{17}\text{O}(\text{N}_2\text{O}_5 - \text{NO}_2)$ $\Delta^{17}\text{O}(\text{NO}_3)_{\text{G3110}} = \Delta^{17}\text{O}(\text{N}_2\text{O}_5 - \text{NO}_3)$
G3201	$\text{NO} + \text{HO}_2 \rightarrow \text{NO}_2 + \text{OH}$	$\Delta^{17}\text{O}(\text{NO}_2)_{\text{G3201}} = 1/2 \left(\Delta^{17}\text{O}(\text{HO}_2) + \Delta^{17}\text{O}(\text{NO}) \right)$
G3204	$\text{NO}_3 + \text{HO}_2 \rightarrow \text{NO}_2 + \text{OH} + \text{O}_2$	$\Delta^{17}\text{O}(\text{NO}_2)_{\text{G3204}} = \Delta^{17}\text{O}(\text{NO}_3)$
G3205	$\text{HONO} + \text{OH} \rightarrow \text{NO}_2 + \text{H}_2\text{O}$	$\Delta^{17}\text{O}(\text{NO}_2)_{\text{G3205}} = \Delta^{17}\text{O}(\text{HONO})$
G3206	$\text{HNO}_3 + \text{OH} \rightarrow \text{H}_2\text{O} + \text{NO}_3$	$\Delta^{17}\text{O}(\text{NO}_3)_{\text{G3206}} = \Delta^{17}\text{O}(\text{HNO}_3)$
G3207	$\text{HNO}_4 (+\text{M}) \rightarrow \text{NO}_2 + \text{HO}_2$	$\Delta^{17}\text{O}(\text{NO}_2)_{\text{G3207}} = \Delta^{17}\text{O}(\text{HNO}_4 - \text{NO}_2)$
G3208	$\text{HNO}_4 + \text{OH} \rightarrow \text{NO}_2 + \text{H}_2\text{O} + \text{O}_2$	$\Delta^{17}\text{O}(\text{NO}_2)_{\text{G3208}} = \Delta^{17}\text{O}(\text{HNO}_4 - \text{NO}_2)$
G4104	$\text{CH}_3\text{O}_2 + \text{NO} \rightarrow \text{HCHO} + \text{NO}_2 + \text{HO}_2$	$\Delta^{17}\text{O}(\text{NO}_2)_{\text{G4104}} = 1/2 \Delta^{17}\text{O}(\text{NO})$
G4105	$\text{CH}_3\text{O}_2 + \text{NO}_3 \rightarrow \text{HCHO} + \text{HO}_2 + \text{NO}_2$	$\Delta^{17}\text{O}(\text{NO}_2)_{\text{G4105}} = \Delta^{17}\text{O}(\text{NO}_3)$
J3101	$\text{NO}_2 + h\nu \rightarrow \text{NO} + \text{O}(^3\text{P})$	$\Delta^{17}\text{O}(\text{NO})_{\text{J3101}} = \Delta^{17}\text{O}(\text{NO}_2)$
J3103a	$\text{NO}_3 + h\nu \rightarrow \text{NO}_2 + \text{O}(^3\text{P})$	$\Delta^{17}\text{O}(\text{NO}_2)_{\text{J3103a}} = \Delta^{17}\text{O}(\text{NO}_3)$
J3103b	$\text{NO}_3 + h\nu \rightarrow \text{NO} + \text{O}_2$	$\Delta^{17}\text{O}(\text{NO})_{\text{J3103b}} = \Delta^{17}\text{O}(\text{NO}_3)$
J3104a	$\text{N}_2\text{O}_5 + h\nu \rightarrow \text{NO}_2 + \text{NO}_3$	$\Delta^{17}\text{O}(\text{NO}_2)_{\text{J3104a}} = 1/5 \left(2\Delta^{17}\text{O}(\text{N}_2\text{O}_5 - \text{NO}_2) + 3\Delta^{17}\text{O}(\text{N}_2\text{O}_5 - \text{NO}_3) \right)$ $\Delta^{17}\text{O}(\text{NO}_3)_{\text{J3104a}} = 1/5 \left(2\Delta^{17}\text{O}(\text{N}_2\text{O}_5 - \text{NO}_2) + 3\Delta^{17}\text{O}(\text{N}_2\text{O}_5 - \text{NO}_3) \right)$
J3200	$\text{HONO} + h\nu \rightarrow \text{OH} + \text{NO}$	$\Delta^{17}\text{O}(\text{NO})_{\text{J3200}} = \Delta^{17}\text{O}(\text{HONO})$
J3201	$\text{HNO}_3 + h\nu \rightarrow \text{OH} + \text{NO}_2$	$\Delta^{17}\text{O}(\text{NO}_2)_{\text{J3201}} = \Delta^{17}\text{O}(\text{HNO}_3)$
J3202	$\text{HNO}_4 + h\nu \rightarrow 0.667\text{NO}_2 + 0.667\text{HO}_2$ $+ 0.333\text{NO}_3 + 0.333\text{OH}$	$\Delta^{17}\text{O}(\text{NO}_2)_{\text{J3202}} = 1/2 \left(\Delta^{17}\text{O}(\text{HNO}_4 - \text{NO}_2) + \Delta^{17}\text{O}(\text{HNO}_4 - \text{HO}_2) \right)$ $\Delta^{17}\text{O}(\text{NO}_3)_{\text{J3202}} = 1/2 \left(\Delta^{17}\text{O}(\text{HNO}_4 - \text{NO}_2) + \Delta^{17}\text{O}(\text{HNO}_4 - \text{HO}_2) \right)$

Modeling of $\Delta^{17}\text{O}$ of NO_x and HO_x

S. Morin et al.

Title Page

Abstract

Introduction

Conclusions

References

Tables

Figures

◀

▶

◀

▶

Back

Close

Full Screen / Esc

Printer-friendly Version

Interactive Discussion



Modeling of $\Delta^{17}\text{O}$ of NO_x and HO_x

S. Morin et al.

[Title Page](#)
[Abstract](#)
[Introduction](#)
[Conclusions](#)
[References](#)
[Tables](#)
[Figures](#)
[◀](#)
[▶](#)
[◀](#)
[▶](#)
[Back](#)
[Close](#)
[Full Screen / Esc](#)
[Printer-friendly Version](#)
[Interactive Discussion](#)


Table 4. $\Delta^{17}\text{O}(\text{X})_i$ for Case 5: Thermal decomposition (TD) scrambling.

Rxn #		$\Delta^{17}\text{O}(\text{X})_i$
G3110	$\text{N}_2\text{O}_5(+\text{M}) \rightarrow \text{NO}_2 + \text{NO}_3$	$\Delta^{17}\text{O}(\text{NO}_2)_{\text{G3110}} = 1/5 \left(2\Delta^{17}\text{O}(\text{N}_2\text{O}_5 - \text{NO}_2) + 3\Delta^{17}\text{O}(\text{N}_2\text{O}_5 - \text{NO}_3) \right)$ $\Delta^{17}\text{O}(\text{NO}_3)_{\text{G3110}} = 1/5 \left(2\Delta^{17}\text{O}(\text{N}_2\text{O}_5 - \text{NO}_2) + 3\Delta^{17}\text{O}(\text{N}_2\text{O}_5 - \text{NO}_3) \right)$
G3207	$\text{HNO}_4(+\text{M}) \rightarrow \text{NO}_2 + \text{HO}_2$	$\Delta^{17}\text{O}(\text{NO}_2)_{\text{G3207}} = 1/2 \left(\Delta^{17}\text{O}(\text{HNO}_4 - \text{NO}_2) + \Delta^{17}\text{O}(\text{HNO}_4 - \text{HO}_2) \right)$ $\Delta^{17}\text{O}(\text{HO}_2)_{\text{G3207}} = 1/2 \left(\Delta^{17}\text{O}(\text{HNO}_4 - \text{NO}_2) + \Delta^{17}\text{O}(\text{HNO}_4 - \text{HO}_2) \right)$

Modeling of $\Delta^{17}\text{O}$ of NO_x and HO_x

S. Morin et al.

Table 5. Diurnally-integrated isotopic signature (DIIS) values for the atmospheric nitrate and H_2O_2 production channels, respectively. Overview of the results from the base model run carried out in springtime (1 April) under mid-latitude (45°N) remote boundary layer conditions.

	$\text{OH}+\text{NO}_2$	NO_3+RH	N_2O_5	HNO_4	H_2O_2
Case 1 – NO_x PSS	20.3	41.6	34.6	15.7	0.0
Case 2 – NO_x explicit	20.3	39.8	32.8	15.7	0.0
Case 3 – HO_x explicit	20.4	39.8	32.8	16.3	1.1
Case 4 – MIF in $\text{H}+\text{O}_2$	20.5	39.8	32.9	16.6	1.8
Case 5 – TD scrambling	19.6	37.1	30.6	15.9	1.4
Case 6 – $\text{OH}+\text{H}_2\text{O}$ IE	20.5	39.8	32.8	16.3	1.1

[Title Page](#)
[Abstract](#)
[Introduction](#)
[Conclusions](#)
[References](#)
[Tables](#)
[Figures](#)
[I◀](#)
[▶I](#)
[◀](#)
[▶](#)
[Back](#)
[Close](#)
[Full Screen / Esc](#)
[Printer-friendly Version](#)
[Interactive Discussion](#)


Modeling of $\Delta^{17}\text{O}$ of NO_x and HO_x

S. Morin et al.

Table 6. Diurnally-integrated source isotopic signature (DIIS) for the four nitrate and H_2O_2 production channels considered. Overview of the results from three model runs carried out at different periods of the year (W=1 January, Sp.=1 April and Su.=1 July, respectively), under mid-latitude (45°N) remote boundary layer conditions.

	$\text{OH}+\text{NO}_2$			NO_3+RH			N_2O_5			HNO_4			H_2O_2		
	W	Sp.	Su.	W	Sp.	Su.	W	Sp.	Su.	W	Sp.	Su.	W	Sp.	Su.
Case 1 – NO_x PSS	24.9	20.3	17.3	41.7	41.6	41.3	34.7	34.6	34.4	18.8	15.7	13.6	0.0	0.0	0.0
Case 2 – NO_x explicit	24.9	20.3	17.3	40.4	39.8	39.2	33.4	32.8	32.3	18.8	15.7	13.6	0.0	0.0	0.0
Case 3 – HO_x explicit	24.9	20.4	17.4	40.4	39.8	39.2	33.4	32.8	32.3	19.3	16.3	14.1	1.0	1.1	0.9
Case 4 – MIF in $\text{H}+\text{O}_2$	25.0	20.5	17.5	40.4	39.8	39.2	33.5	32.9	32.3	19.7	16.6	14.5	1.7	1.8	1.6
Case 5 – TD scrambling	24.2	19.6	16.7	37.3	37.1	37.0	30.9	30.6	30.4	19.9	15.9	13.7	2.8	1.4	1.0
Case 6 – $\text{OH}+\text{H}_2\text{O}$ IE	25.1	20.5	17.5	40.4	39.8	39.2	33.4	32.8	32.3	19.3	16.3	14.1	1.0	1.1	0.9

[Title Page](#)
[Abstract](#)
[Introduction](#)
[Conclusions](#)
[References](#)
[Tables](#)
[Figures](#)
[◀](#)
[▶](#)
[◀](#)
[▶](#)
[Back](#)
[Close](#)
[Full Screen / Esc](#)
[Printer-friendly Version](#)
[Interactive Discussion](#)


Modeling of $\Delta^{17}\text{O}$ of NO_x and HO_x

S. Morin et al.

Table 7. Comparison of diurnally-integrated source isotopic signature (DIIS) for the four nitrate and H_2O_2 production channels considered under mid-latitude (45°N , 293 K) and Arctic (80°N , 253 K) conditions in springtime (1 April).

	$\text{OH}+\text{NO}_2$		NO_3+RH		N_2O_5		HNO_4		H_2O_2	
	45°N	80°N	45°N	80°N	45°N	80°N	45°N	80°N	45°N	80°N
Case 1 – NO_x PSS	20.3	26.0	41.6	41.1	34.6	33.9	15.7	19.6	0.0	0.0
Case 2 – NO_x explicit	20.3	25.9	39.8	40.3	32.8	33.2	15.7	19.5	0.0	0.0
Case 3 – HO_x explicit	20.4	25.9	39.8	40.3	32.8	33.2	16.3	19.9	1.1	0.8
Case 4 – MIF in $\text{H}+\text{O}_2$	20.5	26.0	39.8	40.4	32.9	33.3	16.6	20.3	1.8	1.5
Case 5 – TD scrambling	19.6	24.9	37.1	35.2	30.6	28.0	15.9	21.1	1.4	3.7
Case 6 – $\text{OH}+\text{H}_2\text{O}$ IE	20.5	27.9	39.8	40.3	32.8	33.2	16.3	19.9	1.1	0.9

Title Page

Abstract

Introduction

Conclusions

References

Tables

Figures

I◀

▶I

◀

▶

Back

Close

Full Screen / Esc

Printer-friendly Version

Interactive Discussion



Modeling of $\Delta^{17}\text{O}$ of NO_x and HO_x

S. Morin et al.

Table 8. Comparison of diurnally-integrated source isotopic signature (DIIS) for for the four nitrate and H_2O_2 production channels considered, respectively under mid-latitude (45°N , 293K) and under starting NO_x levels of 20 pmol mol^{-1} (base) and $2\text{ }\mu\text{mol mol}^{-1}$ (high NO_x) in spring-time (1 April).

	$\text{OH}+\text{NO}_2$		NO_3+RH		N_2O_5		HNO_4		H_2O_2	
	base	high NO_x	base	high NO_x	base	high NO_x	base	high NO_x	base	high NO_x
Case 1 – NO_x PSS	20.3	17.3	41.6	41.1	34.6	33.9	15.7	17.5	0.0	0.0
Case 2 – NO_x explicit	20.3	17.3	39.8	40.3	32.8	33.2	15.7	17.5	0.0	0.0
Case 3 – HO_x explicit	20.4	17.4	39.8	40.3	32.8	33.2	16.3	18.1	1.1	1.2
Case 4 – MIF in $\text{H}+\text{O}_2$	20.5	17.5	39.8	40.4	32.9	33.3	16.6	18.5	1.8	1.8
Case 5 – TD scrambling	19.6	16.7	37.1	35.2	30.6	28.0	15.9	19.6	1.4	4.4
Case 6 – $\text{OH}+\text{H}_2\text{O}$ IE	20.5	17.5	39.8	40.3	32.8	33.2	16.3	18.1	1.1	1.2

[Title Page](#)
[Abstract](#)
[Introduction](#)
[Conclusions](#)
[References](#)
[Tables](#)
[Figures](#)
[Back](#)
[Close](#)
[Full Screen / Esc](#)
[Printer-friendly Version](#)
[Interactive Discussion](#)


Modeling of $\Delta^{17}\text{O}$ of NO_x and HO_x

S. Morin et al.

[Title Page](#)[Abstract](#)[Introduction](#)[Conclusions](#)[References](#)[Tables](#)[Figures](#)[I◀](#)[▶I](#)[◀](#)[▶](#)[Back](#)[Close](#)[Full Screen / Esc](#)[Printer-friendly Version](#)[Interactive Discussion](#)

Table 9. Comparison between the DIIS values for $\text{OH}+\text{NO}_2$ and NO_3+RH with the corresponding values assigned to these reaction rates by Alexander et al. (2009). The values deduced from the algorithm presented by Alexander et al. (2009) are compared to DIIS values computed using Cases 1 and 3, under the conditions of the base model run (mid-latitudes).

	$\text{OH}+\text{NO}_2$		NO_3+RH	
	this study	Alexander et al. 2009	this study	Alexander et al. 2009
Case 1 – NO_x PSS	20.3	19.3	41.6	41.4
Case 3 – HO_x and NO_x explicit	20.4		39.8	

Modeling of $\Delta^{17}\text{O}$ of NO_x and HO_x

S. Morin et al.

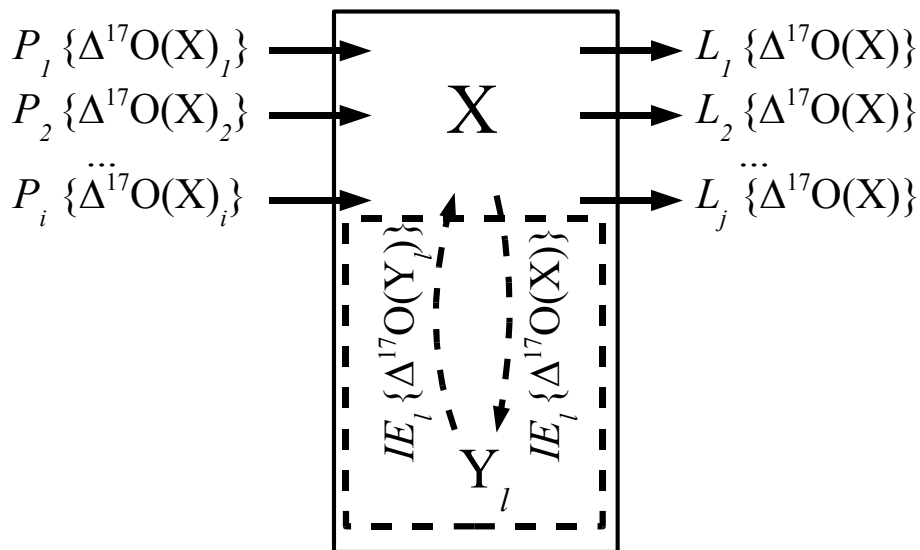


Fig. 1. Schematic representing the isotopic mass-balance equation including one isotopic exchange reaction. Arrows represent production (or destruction) fluxes. The flux is given by the P , L and IE terms, while the corresponding transferred $\Delta^{17}\text{O}$ value is given in brackets. The solid box represent the chemical budget of the species X , while the dashed box takes into account the full isotopic budget of the species X . The scheme illustrates that isotopic exchange reactions have no impact on the chemical budget of a given specie X .

[Title Page](#)
[Abstract](#)
[Introduction](#)
[Conclusions](#)
[References](#)
[Tables](#)
[Figures](#)
[◀](#)
[▶](#)
[◀](#)
[▶](#)
[Back](#)
[Close](#)
[Full Screen / Esc](#)
[Printer-friendly Version](#)
[Interactive Discussion](#)

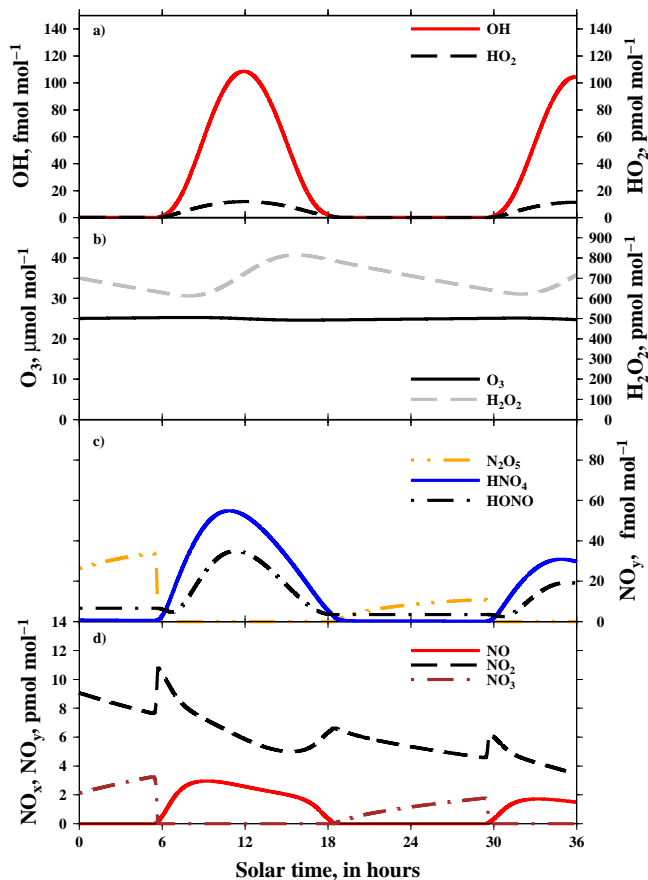



Fig. 2. Time series of the mixing ratio of the main atmospheric species studied, for the base model run ($T=293\text{ K}$, 45° N , see Sect. 3.4 for details). **(a)** OH and HO_2 , **(b)** O_3 and H_2O_2 , **(c)** N_2O_5 , HNO_4 and HONO, **(d)** NO, NO_2 and NO_3 .

Title Page

Abstract

Introduction

Conclusions

References

Tables

Figures

◀

▶

◀

▶

Back

Close

Full Screen / Esc

Printer-friendly Version

Interactive Discussion



Modeling of $\Delta^{17}\text{O}$ of NO_x and HO_x

S. Morin et al.

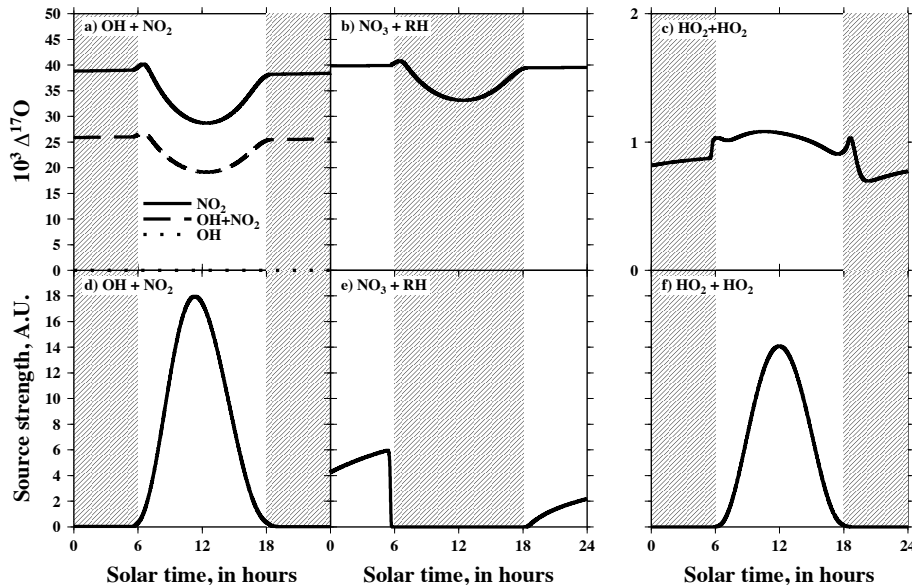


Fig. 3. Simulated diurnal variations of the isotopic signature (a–c) and the strength (d–f) of the OH+NO₂, NO₃+RH nitrate production channel and H₂O₂ production channel, respectively. Note that in the case of the OH+NO₂ reaction, the $\Delta^{17}\text{O}$ values of individual precursors (OH and NO₂) are shown along with the isotopic signature of this reaction channel (see Sect. 2.4.1). Results originate from the base model run ($T=293\text{ K}$, 45° N , see Sect. 3.4 for details) under the isotopic hypotheses of Case 3 (see Sect. 3.2.3). Hatched areas represent the period of the day when the considered reaction pathway proceeds insignificantly, thus the corresponding $\Delta^{17}\text{O}$ which could then be transferred to the reaction products is irrelevant. The diurnally-integrated isotopic source (DIIS) values correspond to the average of values from the upper panel, weighted by the values of the lower one.

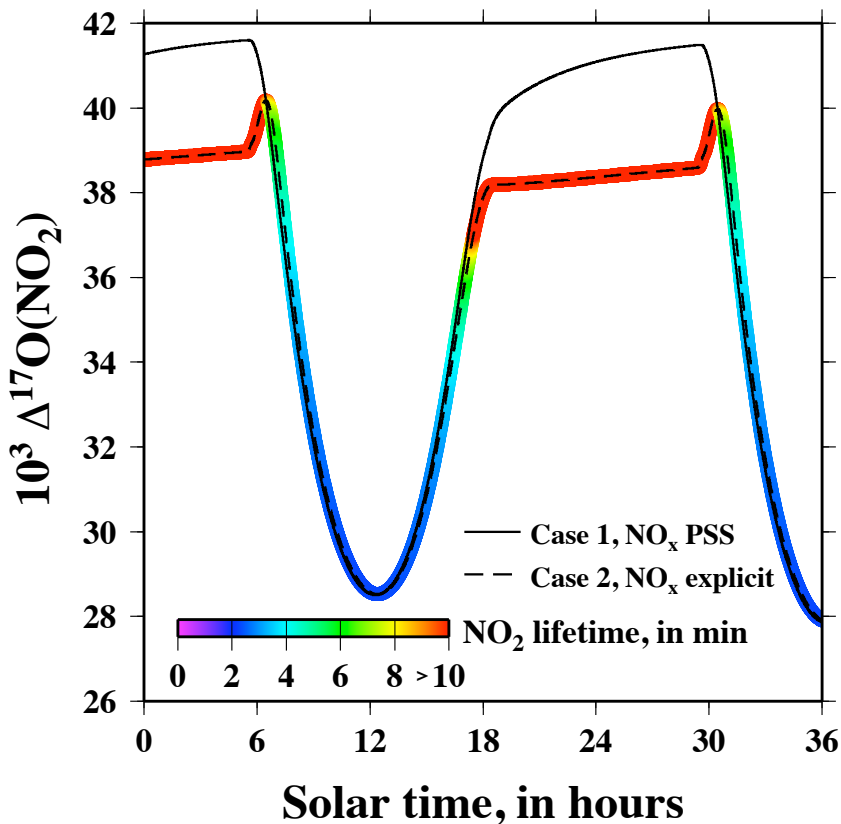


Fig. 4. Diurnal variation of $\Delta^{17}\text{O}(\text{NO}_2)$ calculated using two different approaches, i.e. permanent photochemical steady-state for NO_x (Case 1, solid line) and the explicit computation of $\Delta^{17}\text{O}(\text{NO}_x)$ (Case 2, dashed line). The dashed line representing the results of the simulations under Case 2 is overlaid with a color code exhibiting the diurnal variation of the photolytical lifetime of NO_2 . All values above 10 min are shown in red (at night, the photochemical lifetime of NO_2 is virtually infinite).

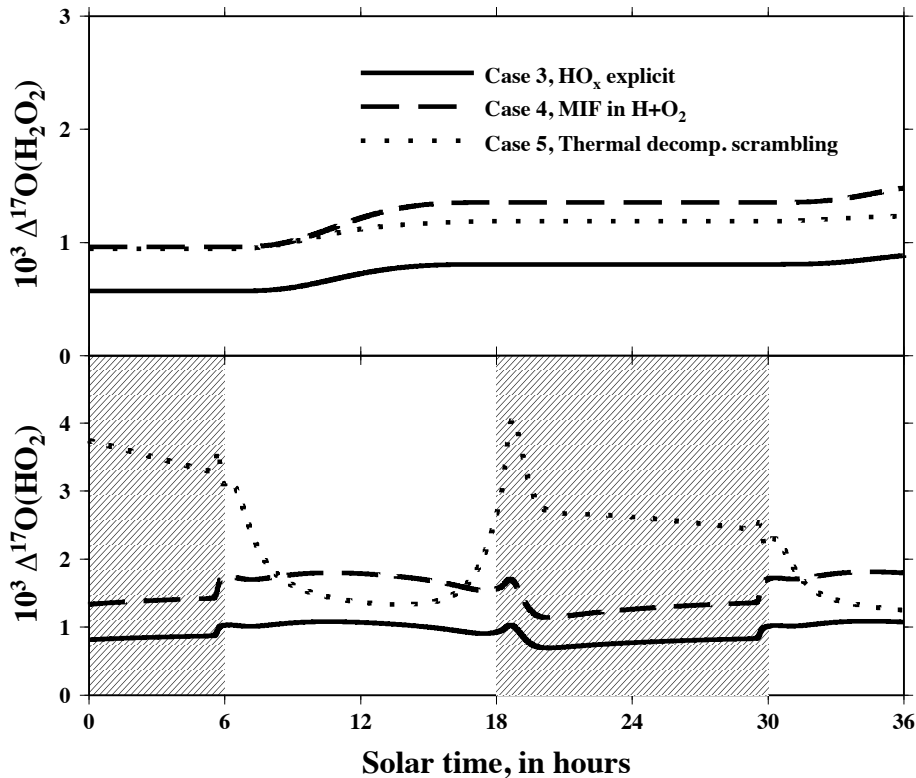


Fig. 5. Simulated diurnal variations of $\Delta^{17}\text{O}(\text{H}_2\text{O}_2)$ (top) and $\Delta^{17}\text{O}(\text{HO}_2)$ (bottom) under the various hypotheses tested, from the results of the base model run. Note that in Case 1 and 2, $\Delta^{17}\text{O}(\text{HO}_2)$ is set to 0. The hatched area covers night-time periods when the presence of HO_2 in the atmosphere is insignificant, hence the relevance of its $\Delta^{17}\text{O}$ value.

Title Page	
Abstract	Introduction
Conclusions	References
Tables	Figures
◀	▶
◀	▶
Back	Close
Full Screen / Esc	
Printer-friendly Version	
Interactive Discussion	

